U.S. Department
of Transportation

**Federal Railroad
Administration**

In-Track Demonstration of Laser-Treated Rail to Reduce Friction and Wear

Office of Research and
Development
Washington, DC 20590

DOT/FRA/ORD-07/17

May 2007

REPORT DOCUMENTATION PAGE

Form approved
OMB No. 0704-0188

1. AGENCY USE ONLY *(Leave blank)*	2. REPORT DATE	3. REPORT TYPE AND DATES COVERED
	May 2007	

4. TITLE AND SUBTITLE
In-Track Demonstration of Laser-Treated Rail to Reduce Friction and Wear

5. FUNDING NUMBERS
DTFR 53-00-C-00012
Task Order 226

6. AUTHOR(S)
Richard Reiff

7. PERFORMING ORGANIZATION NAME(S) AND ADDRESS(ES)
Transportation Technology Center, Inc.
P.O. Box 11130
Pueblo, CO 81001

8. PERFORMING ORGANIZATION REPORT NUMBERS

9. SPONSORING/MONITORING AGENGY NAME(S) AND ADDRESS(ES)
U.S. Department of Transportation
Federal Railroad Administration
Office of Research and Development, MS 20
1120 Vermont Avenue, NW
Washington, DC 20590

10. SPONSORING/MONITORING AGENCY REPORT NUMBER
DOT/FRA/ORD-07/17

11. SUPPLEMENTARY NOTES

12a. DISTRIBUTION/AVAILABILITY STATEMENT
This document is available through National Technical Information Service, Springfield, VA 22161.

12b. DISTRIBUTION CODE

13. ABSTRACT

In-track evaluations of a laser-treated rail intended to provide a permanent reduction of the friction level and increased wear life were conducted at the Transportation Technology Center's Facility for Accelerated Service Testing, Heavy Axle Load track in Pueblo, CO. These evaluations were conducted during the October 2005 operating period. Results suggest that the cracks formed during the laser treatment process led to early spalling and chipping of the gage corner, requiring removal of the test rail from the track. Limited data suggests that the treatment process did not significantly reduce gage face rolling friction.

14. SUBJECT TERMS
Laser-glazed rail, laser-treated rail, spalling, and chipping

15. NUMBER OF PAGES
67

16. PRICE CODE

17. SECURITY CLASSIFICATION	18. SECURITY CLASSIFICATION OF THIS PAGE	19. SECURITY CLASSIFICATION OF ABSTRACT	20. LIMITATION OF ABSTRACT
UNCLASSIFIED	UNCLASSIFIED	UNCLASSIFIED	

NSN 7540-01-280-5500

Standard Form 298 (Rec. 2-89)
Prescribed by ANSI/NISO Std. 239.18
298-102

METRIC CONVERSION FACTORS

Approximate Conversions to Metric Measures

Symbol	When You Know	Multiply by	To Find	Symbol
		LENGTH		
in	inches	*2.50	centimeters	cm
ft	feet	30.00	centimeters	cm
yd	yards	0.90	meters	m
mi	miles	1.60	kilometers	km
		AREA		
in^2	square inches	6.50	square centimeters	cm^2
ft^2	square feet	0.09	square meters	m^2
yd^2	square yards	0.80	square meters	m^2
mi^2	square miles	2.60	square kilometers	km^2
	acres	0.40	hectares	ha
		MASS (weight)		
oz	ounces	28.00	grams	g
lb	pounds	0.45	kilograms	kg
	short tons (2000 lb)	0.90	tonnes	t
		VOLUME		
tsp	teaspoons	5.00	milliliters	ml
Tbsp	tablespoons	15.00	milliliters	ml
fl oz	fluid ounces	30.00	milliliters	ml
c	cups	0.24	liters	l
pt	pints	0.47	liters	l
qt	quarts	0.95	liters	l
gal	gallons	3.80	liters	l
ft^3	cubic feet	0.03	cubic meters	m^3
yd^3	cubic yards	0.76	cubic meters	m^3
		TEMPERATURE (exact)		
°F	Fahrenheit temperature	5/9 (after subtracting 32)	Celsius temperature	°C

* 1 in. = 2.54 cm (exactly)

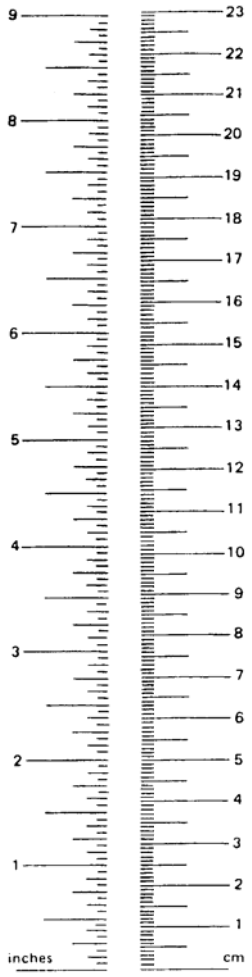

Approximate Conversions from Metric Measures

Symbol	When You Know	Multiply by	To Find	Symbol
		LENGTH		
mm	millimeters	0.04	inches	in
cm	centimeters	0.40	inches	in
m	meters	3.30	feet	ft
m	meters	1.10	yards	yd
km	kilometers	0.60	miles	mi
		AREA		
cm^2	square centim.	0.16	square inches	in^2
m^2	square meters	1.20	square yards	yd^2
km^2	square kilom.	0.40	square miles	mi^2
ha	hectares (10,000 m^2)	2.50	acres	
		MASS (weight)		
g	grams	0.035	ounces	oz
kg	kilograms	2.2	pounds	lb
t	tonnes (1000 kg)	1.1	short tons	
		VOLUME		
ml	milliliters	0.03	fluid ounces	fl oz
l	liters	2.10	pints	pt
l	liters	1.06	quarts	qt
l	liters	0.26	gallons	gal
m^3	cubic meters	36.00	cubic feet	ft^3
m^3	cubic meters	1.30	cubic yards	yd^3
		TEMPERATURE (exact)		
°C	Celsius* temperature	9/5 (then add 32	Fahrenheit temperature	°F

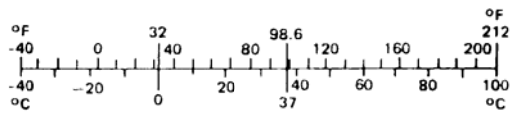

Table of Contents

List of Figures

List of Tables

EXECUTIVE SUMMARY

In-track evaluations of a laser-treated rail intended to provide a permanent reduction of the friction level and increased wear life were conducted at the Transportation Technology Center's (TTC) Facility for Accelerated Service Testing (FAST), Heavy Axle Load (HAL) track in Pueblo, CO, during the October 2005 operating period. Results suggest that the cracks formed during the laser treatment process led to early spalling and chipping of the gage corner, requiring removal of the test rail from the track. Limited data suggests that the treatment process did not significantly reduce gage face rolling friction.

The limited time in track and small (5.6 million gross tons (MGT)) exposure to traffic was insufficient to obtain accurate wear data; thus the effectiveness of this process to control rail wear was not evaluated. While measurements did show dramatic increases in hardness of the laser-treated areas (from 360 Bhn to over 650 Bhn), the depth and thickness of this hardened layer could not withstand continued rolling loads of passing wheels.

Future development of the laser concept must consider the tendency for cracks to develop during the treatment process. Any future laser-treated rail being considered for installation into track must be inspected for cracks. Surface cracking can be easily identified using dye penetrant and magnetic particle inspections. As some of these cracks are very small and occur in the subsurface, however, a metallurgical evaluation of samples cut from production laser-treated segments should also be conducted. This is to ensure that no hidden defects could develop into larger cracks or spalls and chips.

1.0 Introduction

1.1 Background

Railroads utilize a number of lubricant materials and application methods to reduce friction at the wheel/rail contact patch. Data has shown that by proper application of friction controlling materials, rail and wheel wear life can be extended, and energy needed to move a train can be reduced. This has generally been achieved by applying lubricants to the rail's gage face. Lubricants have been applied by a number of methods (mobile-and wayside-based); however, due to the limited life of lubricants once applied to the rail, the application is for every train passing a given location (wayside-based system) or must be applied virtually along the entire route, usually with systems mounted on locomotives (mobile-based systems). For the purposes of this project, an alternative to using lubricants that generally reduce gage face friction to levels of 0.25 μ or less is being considered. Other types of friction control products, which are intended to be applied to the top of rail, are also in use but were not considered for this project.

This project has evaluated a concept that treats the rail gage face and is intended to provide a permanent reduction of the friction level (generally less than 0.25 μ), thus eliminating the need for constant reapplication of lubricants. By laser treating the rail surface, a hard surface is created, which is intended to reduce wear and produce a reduced level of friction. While this process has been demonstrated in laboratory settings that simulate the wheel/rail contact conditions, a full-scale demonstration had not been previously conducted. The Federal Railroad Administration (FRA), working with the Department of Energy (DOE), funded the testing of laser-glazed rail at TTC's FAST in Pueblo, CO, conducted during the October 2005 operating period.

2.0 Objectives

The objectives of the laser-glazed rail evaluation were to determine the following:

- Ability of laser treatment to reduce rail friction to 0.25 μ or less
- Ability of the laser treatment to reduce rail wear rates compared to untreated rail
- Long-term surface fatigue performance of the laser-treated surface

3.0 General Project Approach

Favorable review of laboratory test results on the laser-glazing treatment, conducted by the National Research Council of Canada, were provided to FRA and DOE to justify these full-scale tests. Results were encouraging, such that an in-track test was funded to determine performance of a laser-treated rail under full-scale loaded wheels. The test site selected was in a segment of Section 07 of the track at FAST (Figure 1). By using the high rail of this curve, which is a nonlubricated, 5-degree curve, the effectiveness of the laser treatment in reducing rail wear and friction could be assessed. The FAST/HAL program is used to evaluate track and mechanical components under a train consist with 315,000-pound cars that impose between 100 and 125 MGT annually on the track structure.

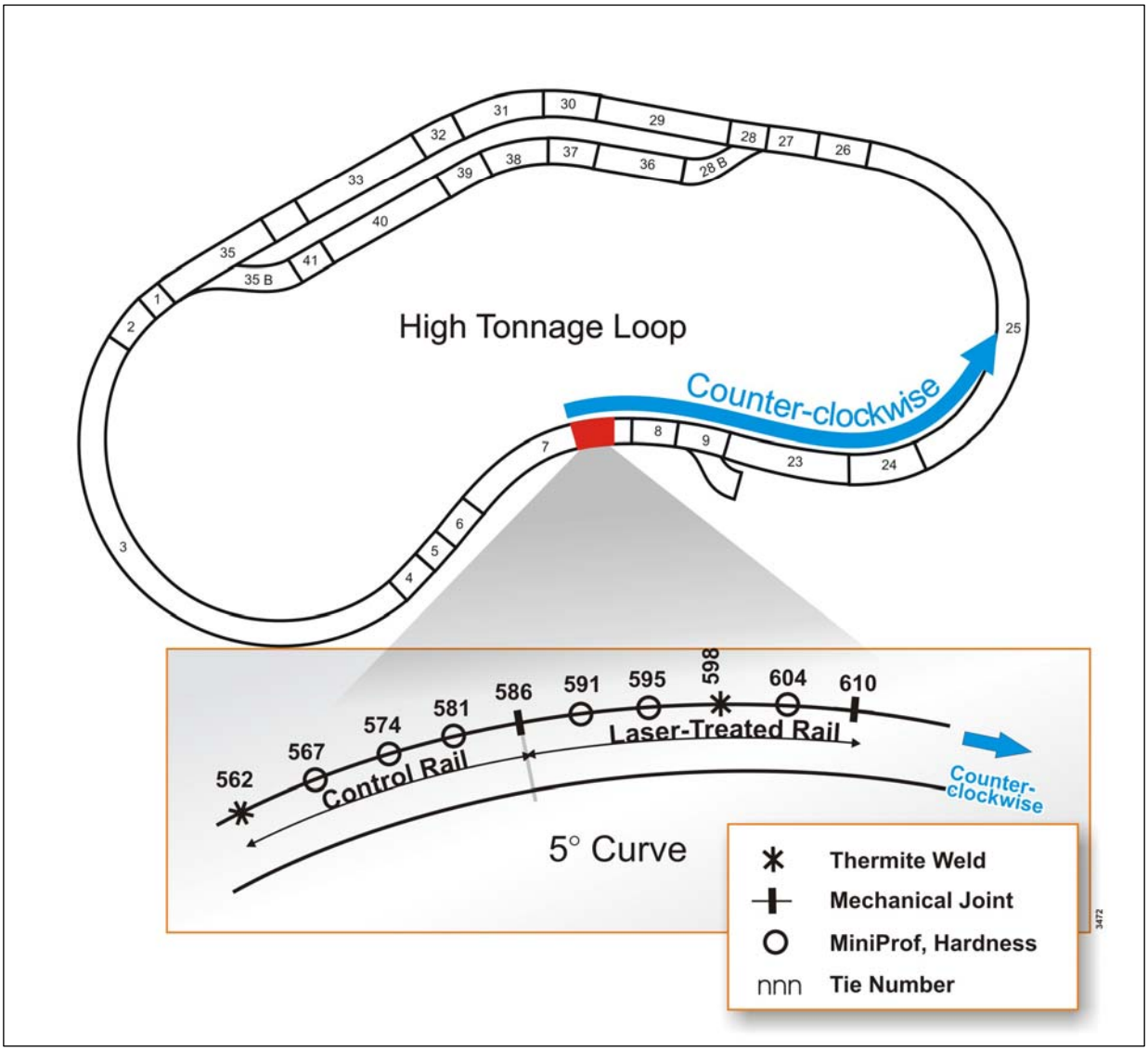

Figure 1. FAST Loop and Location of Test Rail

Normal FAST operations utilize a 4-locomtive/75 (+/-) loaded car train, operating at 40 mph over the 2.7-mile loop. Each loaded car weights approximately 315,000 pounds at the rail. During one 10-hour shift, up to 125 laps can be operated, applying over 1 MGT of traffic. For comparative purposes, a typical North American mainline freight line will be subjected to 60 to 90 MGT per year.

3.1 Test Rail

The Transportation Technology Center, Inc. (TTCI) obtained two 40-foot sections of identical 141 AB (International Steel Group–formerly Pennsylvania Steel Group, heat-treated head hardened (HH) rail) for this test at FAST. One section was kept as is and installed as a control. The other 40-foot section was cut in half and then welded back together to form a 40-foot section containing a thermite weld in the middle. This weld was installed to determine if the laser-treating process would treat the casting-like material of a thermite weld in the same fashion as it does the pearlitic structure of regular rail. Heat-treated rail was selected as almost all major railroads now utilize such rail in curves, as the heat treatment provides superior performance in wear and deformation.

The 40-foot section containing a thermite weld was then shipped to Nuvonyx, near St. Louis, MO, for laser-glazing treatment. Appendix B includes a report of the treatment process. TTCI provided information to Nuvonyx as to the recommended area of treatment, the gage corner area (Figure 2). As this was new, unworn rail, most wheels will contact the rail in the gage corner area.

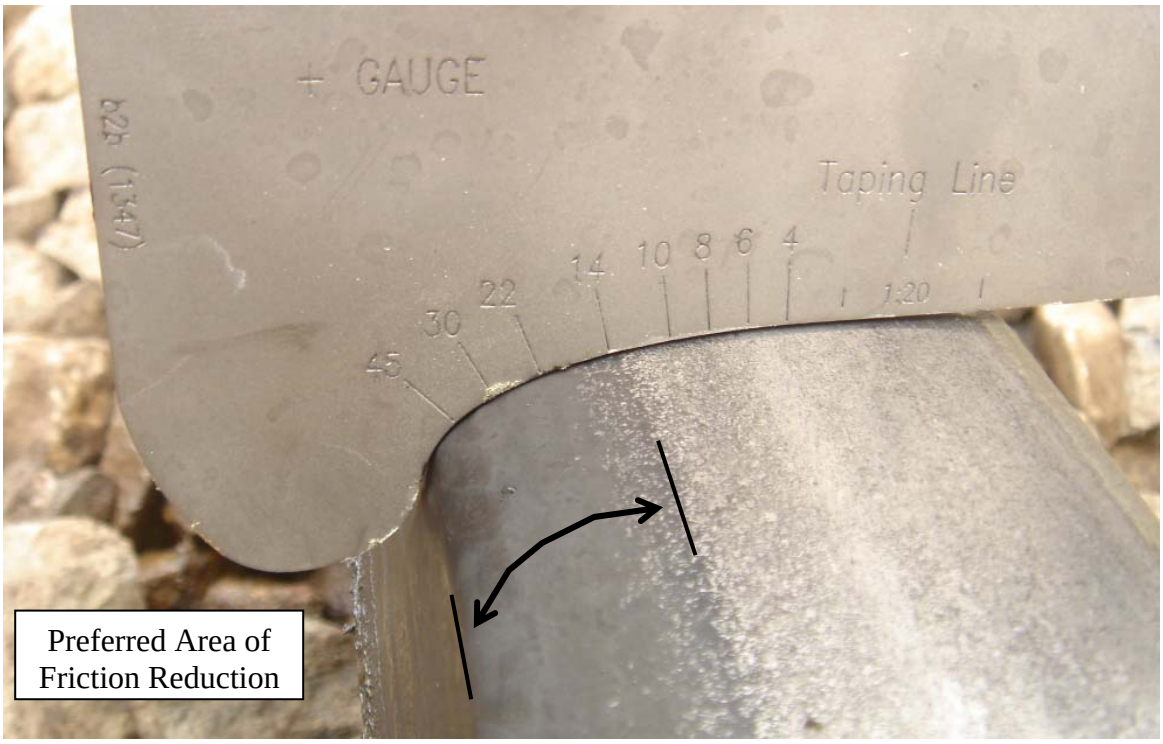

Figure 2. A Typical Rail Showing Dark Grease in Area that Should Have Reduced Friction

3.2 Inspection of Received Rail

Before installation at FAST, the rail was inspected for any major cracking. Figures 3 and 4 show the rail before installation and that the laser-treated surface had a rough appearance.

Figure 3. Overall View of Laser-Treated Rail Before Installation

Figure 4. Closeup of Laser-Treated Rail Before Installation

3.3 Measurements

Because laser glazing of rail is an experimental procedure and its effect on the performance of rail under actual operating conditions was uncertain, to ensure safety, the rail was inspected visually each day following train operations. To determine performance of the laser-treated rail, monitoring locations were established on the control and laser-treated rail. Data included MiniProf™ cross-sectional rail profiles, hardness, and rail friction.

3.3.1 Profiles

A MiniProf™ profile was measured at the beginning of the test and scheduled every 25 MGT after that. Three measurement sites were implemented on the nonglazed section and three on the glazed section. Figure 1 shows these in numbered sequence. Due to premature failure, end-of-test profiles were taken after 5.6 MGT.

3.3.2 Rail Hardness

An Equiotip® Brinell device was utilized to measure rail hardness at the same intervals as rail profile measurements.

3.3.3 Rail Friction

Rail friction was measured with a hand-held tribometer. Due to the need for a distance of 25 to 30 feet for the tribometer to measure, only 1 or 2 friction readings could be taken on either section.

3.3.4 Photo and Other Documentation

Photos were taken to show surface conditions, along with notes and records of train operation and tonnage.

4.0 Installation of Test Rail

After the rail was laser treated, a short section was cut and removed for possible future laboratory analysis. The remaining 39-foot section was then installed in track along with the control rail. The laser-treated rail and control rail were installed at the same time. Rail was then installed on the outside of Section 7 of the High Tonnage Loop (HTL) at FAST, a nonlubricated, 5-degree curve where rail wear tests are conducted (Figure 1).

Figure 5 shows the condition of the rail as installed before any train operations.

Figure 5. Laser-Treated Test Rail as Installed in Section 07 at FAST Before Train Operation

5.0 Results

Before operation, all sites were measured for profiles, hardness, and rail friction. As shown on Table 1, hardness data was potentially impacted due to mill scale present on running surfaces of the control rail. The tribometer data may also have been impacted due to mill scale on the non-laser-treated surfaces. Table 1 shows the hardness of the laser-treated surface is much greater than the control rail that is untreated surface (approximately 670 bhn versus 340 bhn).

Table 1. Notes from Pre-Operation Data Collection

Laser-Glazed Rail Test						
Date: 10/14/05						
MGT: 0 Mgt first test						
Tie Location	**MiniProf™**	**Equio-Tip Hardness**		**Tribo-Reading**		
	File Name	**Top**	**Gage Face**	**Top**	**Corner**	**Face**
07-567	14102005-0011	347	N/A			
07-574	14102005-0021	353	N/A	0.38	0.34	0.25
07-581	14102005-0031	348	N/A			
07-591	14102005-0041	340	680			
07-595	14102005-0051	350	668	0.35	0.32	0.23
07-604	14102005-0061	354	653			
The hardness was taken with de-carb on the running surface. *The tribometer readings were taken with scale and rust on the rail.*						

After approximately 1.2 MGT of operation, the rail was re-inspected and hardness re-measured. Field inspection of the control and laser-treated rail indicated no issues with the control rail; however, the laser-treated rail exhibited several chips and spalls. Table 2 summarizes the results of friction and hardness measurements after one night of train operation.

Table 2. Summary of Hardness and Friction After 1.2 MGT of Traffic at FAST

Laser-Glazed Rail Test						
Date: 10/17/05						
MGT: 1 MGT test						
Tie Location	**MiniProf™**	**Equio-Tip Hardness**		**Tribo-Reading**		
	File Name	**Top**	**Gage Face**	**Top**	**Corner**	**Face**
07-567	None	353	N/A			
07-574	None	350	N/A	48	31	30
07-581	None	341	N/A			
07-591	None	360	658			
07-595	None	346	650	48	32	30
07-604	None	368	650			
The laser rail still rough. Tribo still has a hard time giving a correct reading.						

Figure 6 shows the control rail after 1.2 MGT of traffic. Figures 6 through 12 document the visual inspections conducted after 1.2 MGT of traffic.

Figure 6. Control Rail After 1.2 MGT. Compare with Figures 14 and 15, Same Location After 5.6 MGT

Figures 7 through 12 show the laser-treated rail surface conditions after 1.2 MGT of traffic. In Figure 7, note the smoothed gage corner, where most of the wheel contact appears to have occurred as compared to Figures 3 and 4, which show the gage corner before operating any trains and show no wear on the rail.

Figure 7. View Along Gage Corner, Looking in the Clockwise Direction After 1.2 MGT

Figure 8. Typical Chip Noted on Gage Corner of Laser-Treated Trail After 1.2 MGT

Figure 9. Two Chips on Gage Corner of Laser-Treated Rail After 1.2 MGT Compare with Figure 17 at the Same Location After 5.6 MGT

Figure 10. Closeup of the Same Location as Shown in Figure 9 After 1.2 MGT. Compare with Figure 17 on the Same Location After 5.6 MGT to Show Growth in Size of Spalling

Figure 11. Overall View of Thermite Weld in Laser-Treated Section After 1.2 MGT. Compare with Figure 19 at the Same Location After 5.6 MGT

Figure 12. Closeup View of Thermite Weld (as Shown in Figure 11) in Laser-Treated Section After 1.2 MGT. Compare with Figure 20 at the Same Location After 5.6 MGT

Information regarding chipping was transmitted to the sponsors and developers of this concept. After the fourth night of operation (5.6 MGT), the laser-treated rail exhibited severe spalling (12 spalls noted in the 40-foot length); thus it was decided to remove the rail from track and conduct metallurgical evaluations of the laser-treated surfaces. Although the cracking was not a safety concern at the time, further cracking would have prevented adequate rail flaw detection and reduced system safety.

During the initial 5.6 MGT, tribometer data indicated almost no significant difference between the laser-treated and untreated surfaces, as summarized in Figure 13.

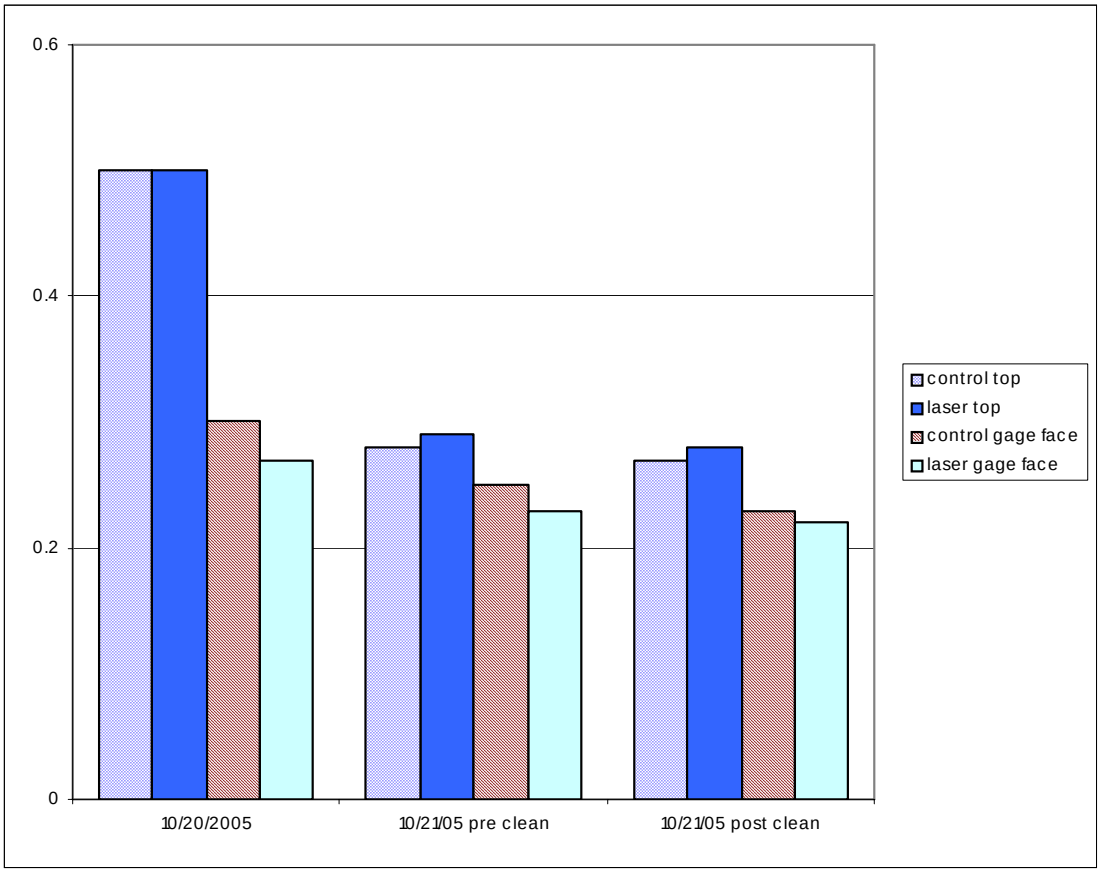

Figure 13. Summary of Tribometer/Friction Data Showing Only a Slight Reduction or No Change Between the Laser-Treated and Untreated Surfaces

Inspection of the control and laser-treated rails after 5.6 MGT of traffic showed the following surface conditions.

Figures 14 and 15 show the condition of the control/untreated rail after 5.6 MGT.

Figure 14. Control Rail Showing Rough Gage Face from Dry Operation. Shiny Gage Corner After 5.6 MGT

Figure 15. Control Rail Closeup Showing Dry Surfaces. No Pitting or Spalling After 5.6 MGT

As a concern existed that the surface condition might develop fatigue failures early in the test, the laser-treated rail was initially bolted in place, with the intent to weld it at both ends to the adjacent rail if no problems occurred. Figure 16 shows the appearance of the mechanical joint at the junction between the control and laser-treated rails after 5.6 MGT. As seen, the left side (center rail) shows no cracking and a smooth surface. The treated rail, to the right of the joint, is rough and shows signs of cracking.

Figure 16. Junction of Control Rail to Laser-Treated Rail.
Left Side is the Control Rail; Right Side is Laser-Treated Rail

Figures 17 through 20 show various locations along the laser-treated rail after 5.6 MGT. Figure 18 shows the smooth gage corner from contact with wheels but with large valleys and rougher surface of laser-treated area. Figure 19 shows spalling at the center and each side of the thermite weld; compare with the same location shown in Figure 11 after 1.2 MGT.

Figure 17. Laser-Treated Rail After 5.6 MGT Showing Two Spalls. Compare with Same Location as Shown in Figures 9 and 10 After 1.2 MGT

Figure 18. Typical View of Gage Corner on Laser-Treated Rail, No Spalls. Compare to Figures 3 and 4, Which Show the Gage Corner Before Train Operation

Figure 19. Thermite Weld on Laser-Treated Rail Segment After 5.6 MGT

Figure 20. Close View of Spalls At and Near Thermite Weld After 5.6 MGT. Compare with Same Location as Shown in Figure 12 After 1.2 MGT

6.0 Laboratory Evaluation of Rail Samples

Due to the premature failure of the laser-treated rail surface, in the form of numerous spalls or cracks that would likely develop into spalls, the rail was removed from the track after 5.6 MGT of traffic. In order to better understand the failure mechanism, a series of laboratory tests was proposed and authorized in lieu of continuing the in-track tests. Appendices A and B include results of the laboratory testing.

TTCI recommends that any future specimens of laser-glazed treated rails undergo a full metallurgical evaluation to determine their integrity before installation in track. No rail should be subjected to HAL traffic, either at FAST or revenue service, with evidence of cracks similar to the ones observed in these rail sections.

7.0 Conclusions and Observations

The rail was removed from track after 5.6 MGT due to numerous spalls that developed along the gage corner area of the laser-treated rail. No spalling or other surface damage was noted on the otherwise identical, untreated control rail. Spalling on the laser-treated rail appeared to grow or originate from cracks created during the treatment process. These cracks were located in the very hard laser-treated material on top of the softer parent metal. Similar hardness transitions occur at engine burns or where improper rail grinding has been conducted, creating small sections of martensite next to the parent metal. At such locations it is common to see chips or spalls break out from the running surface. With the laser-treated rails, however, the cracks were preexisting and led to rapid failure of the rail section.

In the laser-treated rail, the potential for cracks to develop into spalls was not at isolated locations, but along the entire gage face of the rail. For this reason, the rail was removed after 12 large spalls were noted within the 39-foot laser-treated rail length. Additional operation would have likely led to additional spalling and possible safety issues.

One issue that may have accelerated the development of spalls and chipping is that the laser treatment appears to have very slightly altered the rail's profile. Examination of Figure 21 shows an overlay between a new 141 AB rail and the laser-treated 141 AB rail sections. The profile of the glazed/treated rail has minor bumps that are higher than the original profile. These locations likely make more frequent contact with passing wheels and would create much higher contact stresses until they are worn down or away. During the brief 5.6 MGT of exposure to traffic, it appears that many of these bumps resulted in chips and spalls.

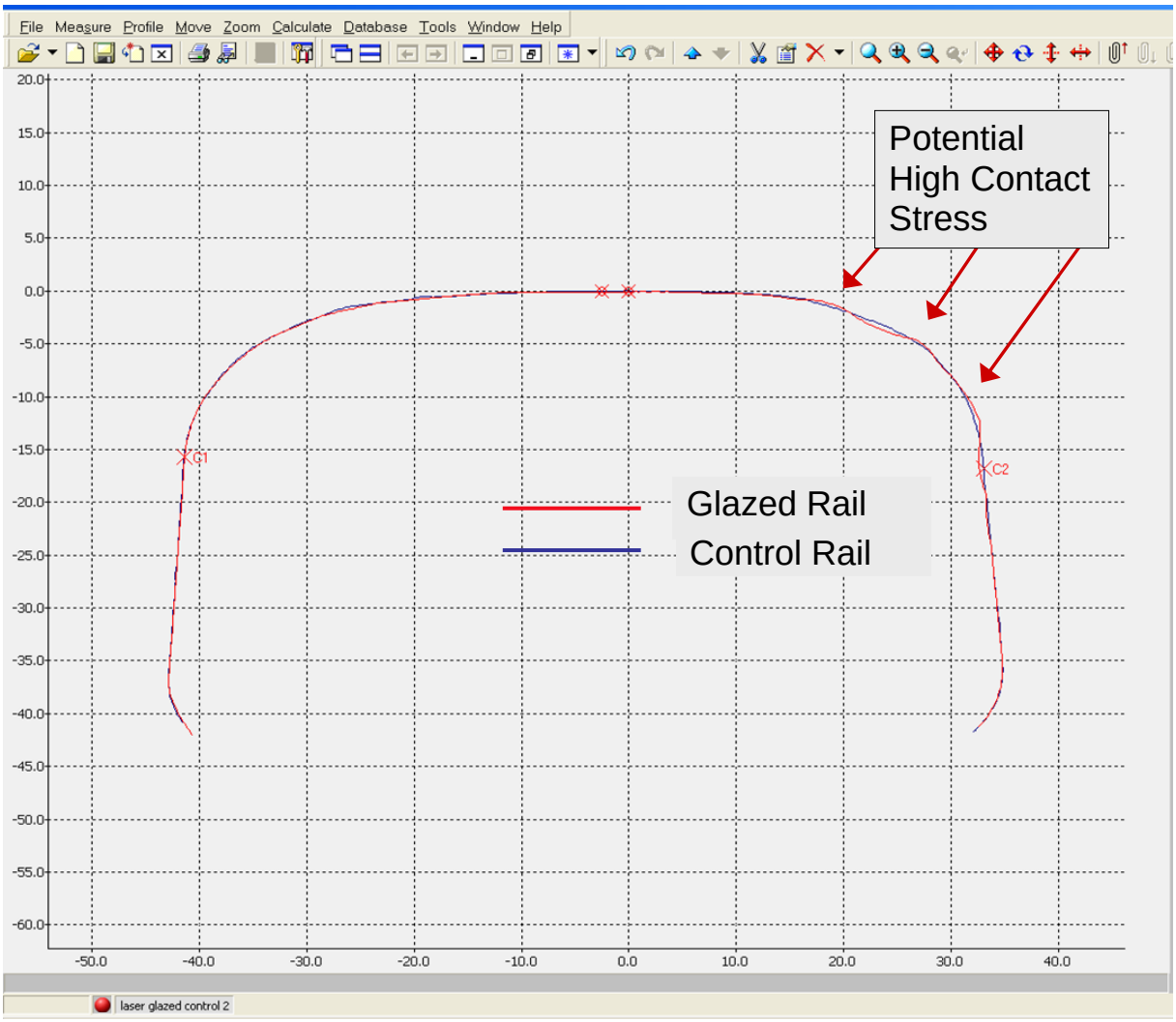

Figure 21. Overlay of Control (untreated) and Laser-Treated Rail

The laser-treated rail, as received, had a very rough surface along the gage face/corner area. Based on laboratory analysis of a sample from the laser treated, unused section, cracks were present within this laser-treated surface. Most of the small cracks, which likely developed during the treatment process, would have eventually grown into large cracks and led to additional spalling and chipping of the rail surface.

The relatively short time of testing did not allow the gage corner/gage face rail surface to become smooth; thus reliable tribometer readings could not be collected. The limited amount of tribometer data obtained shows little or no difference between the control and laser-treated rails, both on the gage face and the top running surface. This suggests that the harder material did not affect the tribometer wheel in the stick-slip mode in the same fashion as grease or oil. Although the laser-treated rail exhibited a smoothed, narrow band along the gage corner that was also smooth to the touch, this did not produce friction levels significantly lower than the adjacent control rail. A dry, unlubricated gage face sometimes produces metal flakes, which can interfere with accurate tribometer readings. These metal flakes act like ball bearings (due to the size factor) and can reduce the measured friction value. An attempt to clean the rail did not, however, result in any increase in readings. In fact, a reduction in friction readings from the tribometer was observed. The cleaning effort may have removed only the larger metal flakes, leaving the small ones in place, resulting in reduced friction values. Again, even after cleaning, the laser treated and control sections did not show any significant difference.

As only 5.6 MGT of operations occurred, measured wear was within the (MiniProf™) measurement system error. In some cases spalling occurred at the location where profiles were to be measured, which would have produced erroneous results. A much longer period (25 MGT or more) would be needed to determine if wear were significantly reduced over the laser-treated segment. With the frequency, depth, and size of spalls, the laser-treated rail gage face would have exhibited large amounts of wear at many locations.

8.0 Future Application and Development

Based on the rough surface condition and the cracks developed during the treatment process, additional refinement of the laser treatment technique is needed to make this concept acceptable for general use in the freight railroad industry. Even small cracks, if not worn away, will grow with applied tonnage and eventually result in spalls or, in the worst case, cracks that turn downward into the rail resulting in breaks. In addition, the rough surface of the gage face makes normal ultrasonic inspection of this surface in the field virtually impossible. Thus inspection for cracks is difficult using routinely utilized inspection equipment. The rough surface is not a rail condition that most railroad personnel will be expecting; thus issues with cracks and inspection must be addressed for this process to be acceptable. Finally, the roughened surface also produced some minor bumps and variations that extend outward from the original profile. These bumps appeared to take the brunt of passing wheel loads and were likely the origin of some of the early spalls. Future processes that treat rail should not change the rail profile shape and should maintain a smoother running surface.

Appendix A.
Laser-Glazed Rail Failure Analysis

By Francisco Hernandez Robles, TTCI Principal Investigator

A-1.0 Background

The Transportation Technology Center, Inc. (TTCI), Pueblo, CO, received a rail sample that had been treated by a laser-glazing process. This sample was installed in the Facility for Accelerated Service Testing (FAST) at the Transportation Technology Center (TTC) in Pueblo, CO, for monitoring under heavy axle load (HAL) traffic (39 tons per axle). Shown in Figure A-1, a visual inspection before installing the rail in track showed possible signs of metallurgical damage in the regions where the rail had been treated with the laser-glazing process. Figure A-2 shows that after approximately 5.6 million gross tons (MGT) of HAL traffic, the glazed areas showed signs of chipping at the rail's gage corner. Since the rail has shown a susceptibility to damage, the Federal Railroad Administration (FRA) and TTCI technical staff decided to remove the rail from the test.

TTCI recommends that before installing any other laser heat-treated rails in track, a metallurgical analysis should be performed on the rail. The analysis will be used to document the metallurgical characteristics of the treated areas on the rail before and after being subjected to HAL traffic.

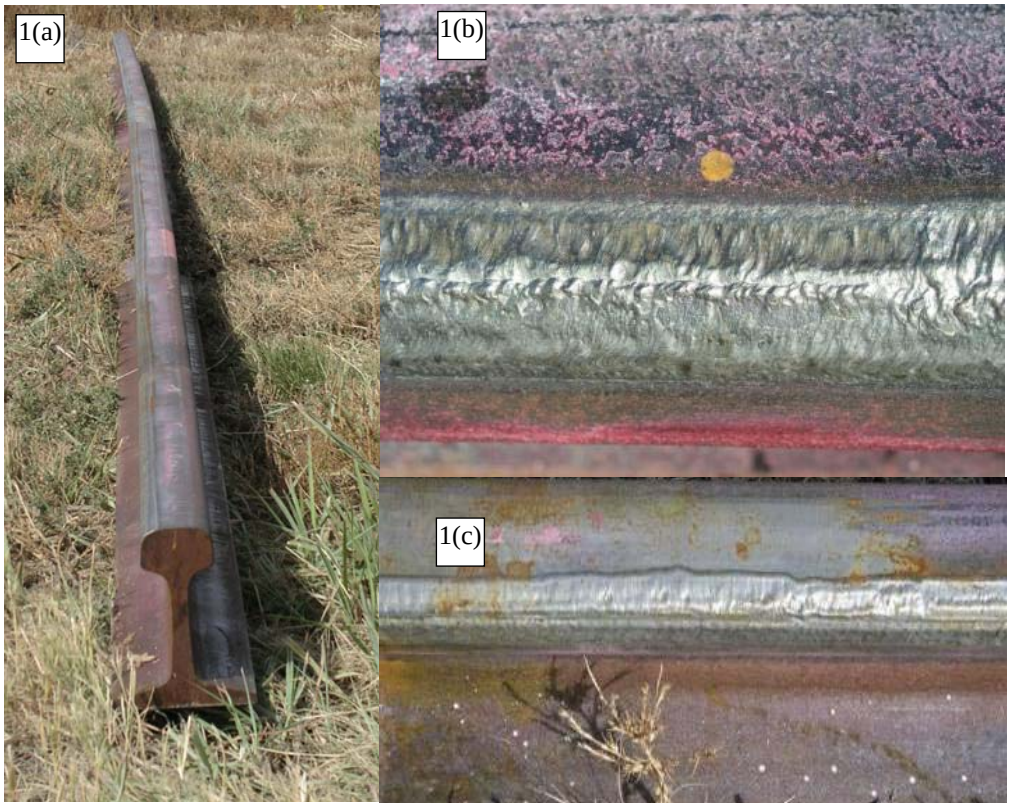

Figure A-1. Figure 1(a). Laser-Glazed Treated Rail, Figure A-1(b). Rough, and Figure A-1(c). Uneven Glazed-Treated Gages for the Untested Rail

Figure A-2. Figure A-2(a) Rail Removed from FAST Facilities After Approximately 5.6 MGT of HAL Traffic, Figure A-2(b). Macro-Picture Showing Severe Wear, and Figure A-2(c). Macro-Picture Showing Shelling Regions of the Laser-Glazed Rail

A-2.0 Non-Destructive Testing (NDT) Analysis

A-2.1 Visual and Non-Destructive Examination (Non-Service Tested Rail)

A 6-foot piece of the rail was cut from the original rail sample. This section was used for the present metallurgical analysis in order to compare the effect of HAL traffic on the integrity of the glazed rail. The visual examination showed no cracks on the glazed regions; however, using magnetic particle and liquid penetrant inspections, several cracks were identified particularly along the regions where the two laser-glazed treatments overlap, as shown in Figures A-3(a) and 3(c). No cracks were revealed in the cross section (Figures A-3(b) and 3(d)) of the rail by NDT techniques.

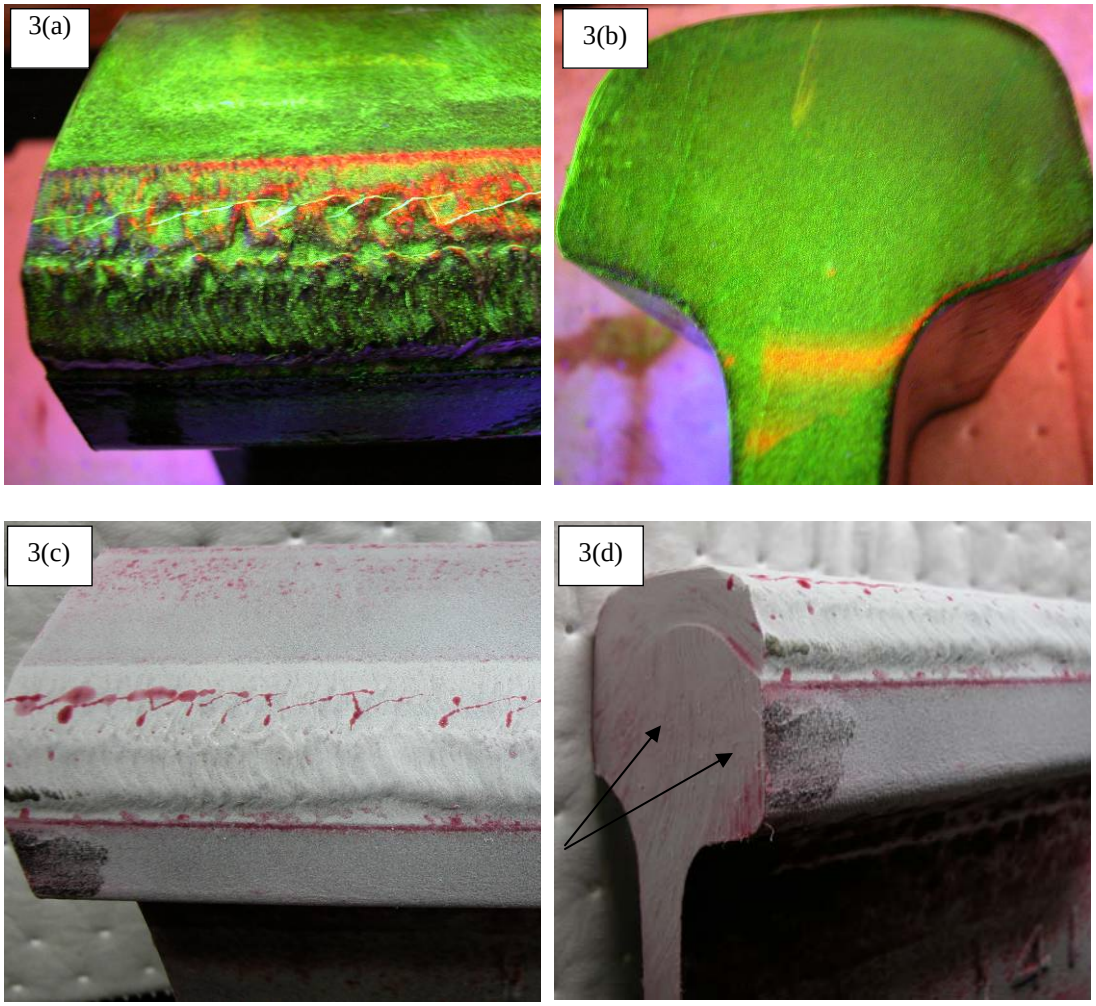

Figure A-3. Figures A-3(a) and 3(b). Macro-Pictures of the Laser-Glazed Rail Analyzed with Magnetic Particles. Figures A-3(c) and 3(d). Liquid Penetrant (Arrows in 3(d) Show Damage Caused with the Cutting Tool)

A-2.2 Visual and Non-Destructive Examination (Service-Tested Rail)

The laser-glazed treated rail was removed from FAST after approximately 5.6 MGT of HAL traffic due to its susceptibility to shelling at the gage corner area (Figure A-2(c)). After the rail was removed from FAST, it was sectioned for analysis at TTC. Three pieces, 3-feet long, were shipped to Argonne National Laboratory. Figure A-4 shows a sketch of the sections of the rail and indicates the locations for sections sent to the Argonne National Laboratory, as well as the ones kept at TTC for analysis. An additional 2-foot portion of control rail was cut and is kept at TTC for future investigations (if required and/or requested). The present metallurgical analysis was conducted on Section V of the rail located between ties 590 and 600, approximately nine feet from either tie (See Figure A-1).

The damage revealed by the NDT of the laser-glazed treated rail removed from FAST shows more severe damage at the gage corners when compared to the non-service tested rail. This damage is the result of increased susceptibility of the laser-glazed treated regions to cracking and shelling. Figure A-5 shows pictures of the magnetic particle analysis of the gage regions and the cross section of the rail. In the cross section of the rail, no cracks were revealed by the NDT methods used.

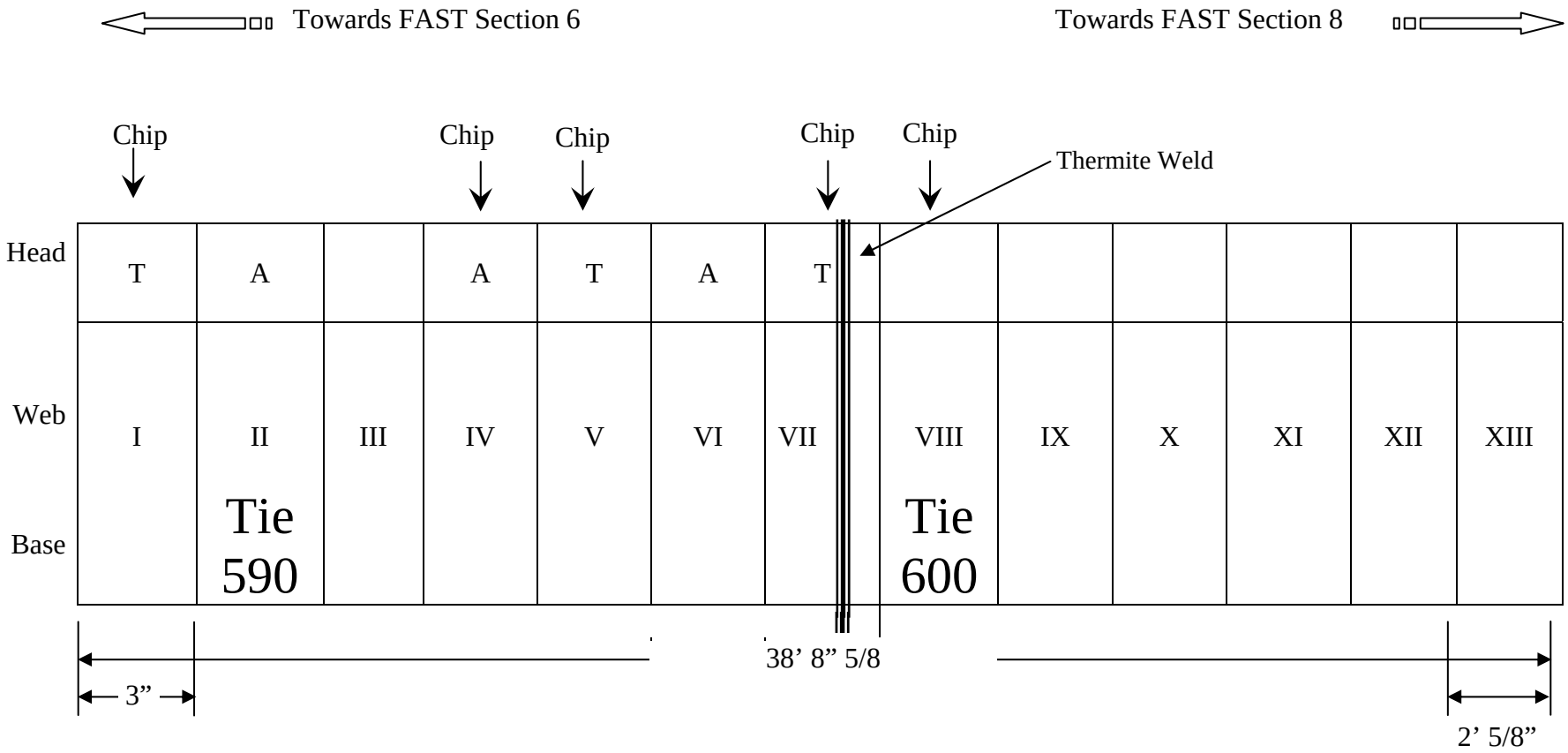

Sections I through XII (identified in the web of the rail) of the laser-glazed rail are 3’ in length, and Section XIII is 2’ 5/8”. Sections VIII through XIII will be kept at TTCI for future reference or analysis unless otherwise requested by Argonne National laboratory.

Head of the rail:

Sections I through VI were used for analysis; the letters on the head of the rail indicate how these sections were distributed:

- *“A” indicates the shipped sections to the Argonne National Laboratory.*
- *“T” indicates the specimens that were analyzed at; Section V was selected for the present metallurgical study.*

Figure A-4. Sketch Showing Segments of Rail Used for Analysis at TTC, as Well as Sections Sent to Argonne National Laboratory

5(a)

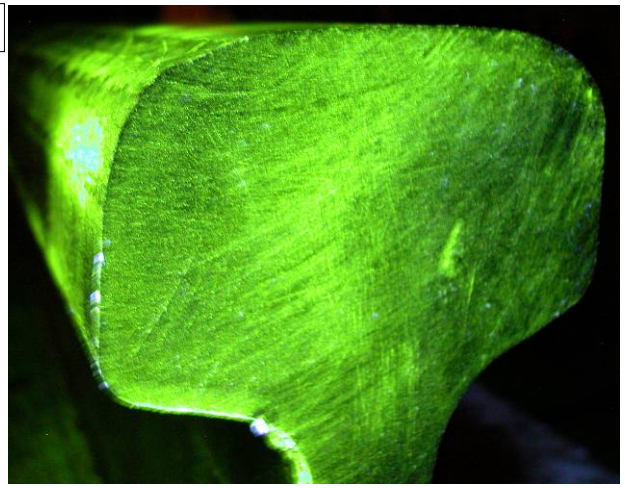

5(b)

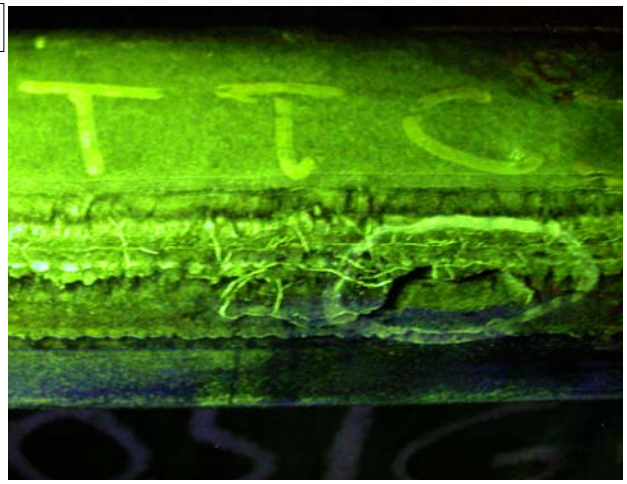

5(c)

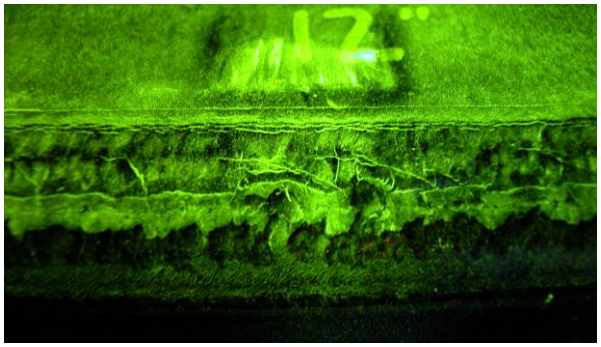

5(d)

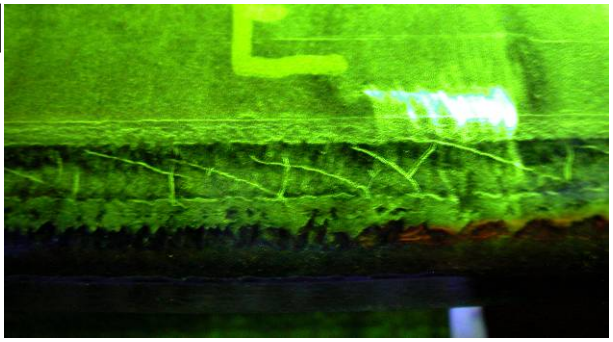

Figure A-5. Photographs of Magnetic Particles Analysis of Various Sections of Laser-Glazed Rail After Removal from FAST at Approximately 5.6 MGT of HAL Traffic Showing No Cracks in Cross Section of Rail.
Figure A-5(a). Section Showing Shelling at the Gage Corner of the Rail.
Figure A-5(b). Extended Cracks Along the Gage Corner of the Rail.
Figures A-5(c) and A-5(d). Compare with Laser-Glazed Non-Service Tested Rail that Presents a Less Severe Damage

A-3.0 Metallurgical Analysis

The metallurgical analysis for the non-service tested rail was conducted on the previously mentioned 6-foot section extracted from the section of the rail sample indicated in Figure A-4, the original laser-glazed rail. The section used for the present metallurgical and NDT analysis was located between ties 590 and 600 (approximately 9 feet from either end tie). In addition, a metallurgical analysis for the untreated (field) corners of the non-service tested and service-tested rails was conducted. Both above-mentioned portions of rail were sectioned to obtain a set of six metallographic samples for each rail condition, three from the gage (laser-glazed) and three from the field sides of the rail. For the service-tested portion of the rail, two of the three samples were cut in close proximity to the shelled region to analyze the sections of the rail containing the most severe damage caused by HAL traffic. In addition, six charpy samples were extracted for every rail condition (service tested and non-service tested); three samples were from the gage corner and the other three from the field corner. Each sample was tested at different temperatures [-30° C (5° F), 0° C (32° F), and 65° C (175° F)] to investigate the effects of the laser-glazed treatment and the HAL traffic on the fracture mechanisms presented on the treated rail under different temperatures (environments).

A-3.1 Stereoscopic Examination

Subsequent to initial visual examination, the metallographic samples were micro-and macro-graphically examined. The metallographic samples were polished following standard procedures. Using the stereo-macroscope on both non-service tested and service-tested samples, several cracks across the glazed regions were identified. A description of the stereo-macroscopic analysis conducted on the metallographic samples follows.

Figures A-6(c) and 6(b) show that for the non-service tested rail, the macrographs of the laser-glazed (gage, Figure A-6(b)) and (field, Figure A-6(c)) sections of the rail. The macrographs were taken at magnifications of 3.5x for Figure A-6(a), 45x for Figure A-6(b), and 3.5x for Figure A-6(c). In the gage side of the rail, cracks were found along the glazed regions. In all cases, the cracks did not propagate past the interface between the glazed region and the parent rail material. In contrast, the field side of the rail did not have cracks present.

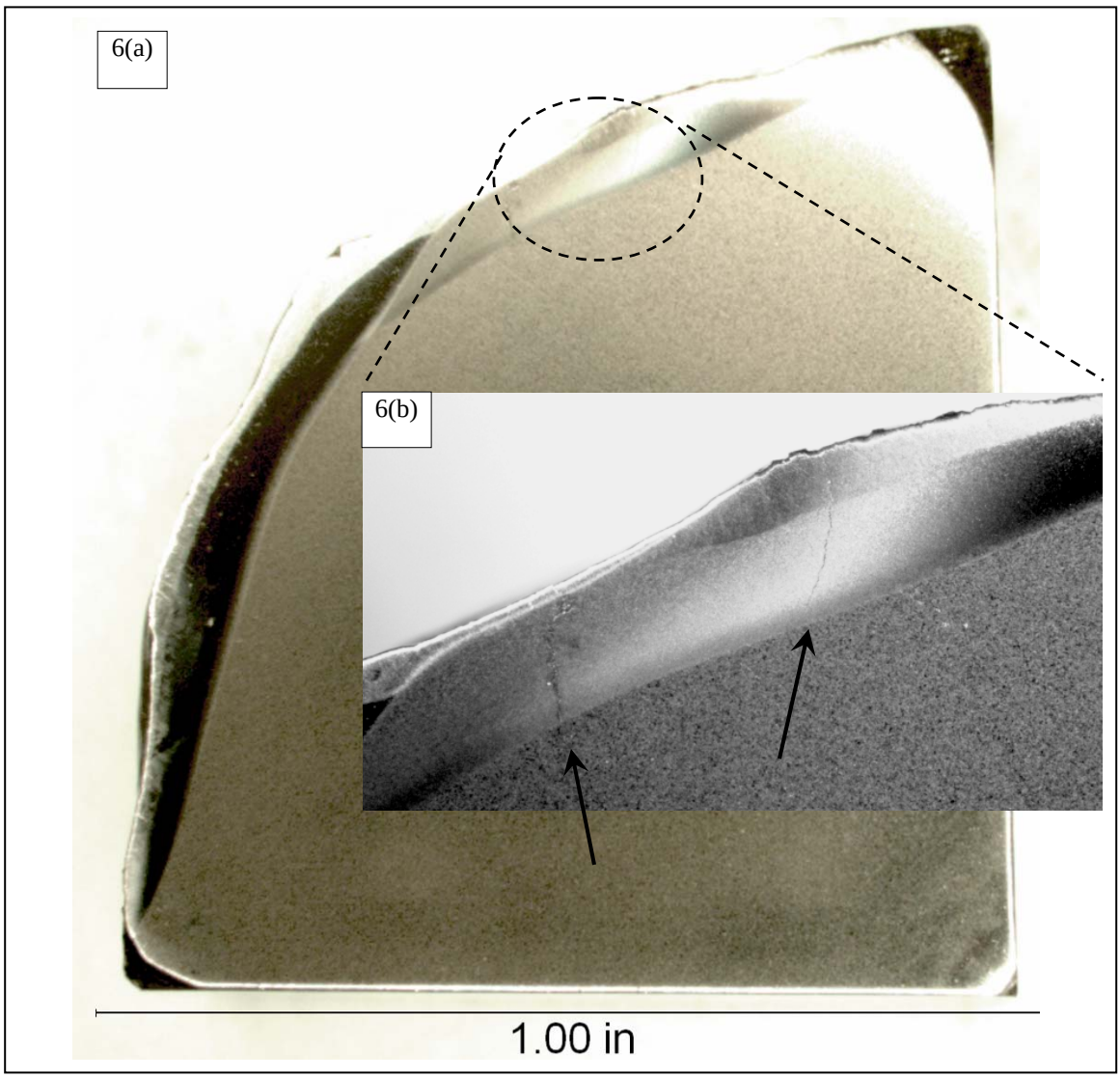

Figure A-6. Macrographs of Laser-Glazed Treated Rail at Gage Corner Showing Cracks Across Glazed Areas. Arrows Point to Cracks.
Figure A-6(a). Macrograph with 3.5x Magnification
Figure A-6(b). Macrograph with 45x Magnification

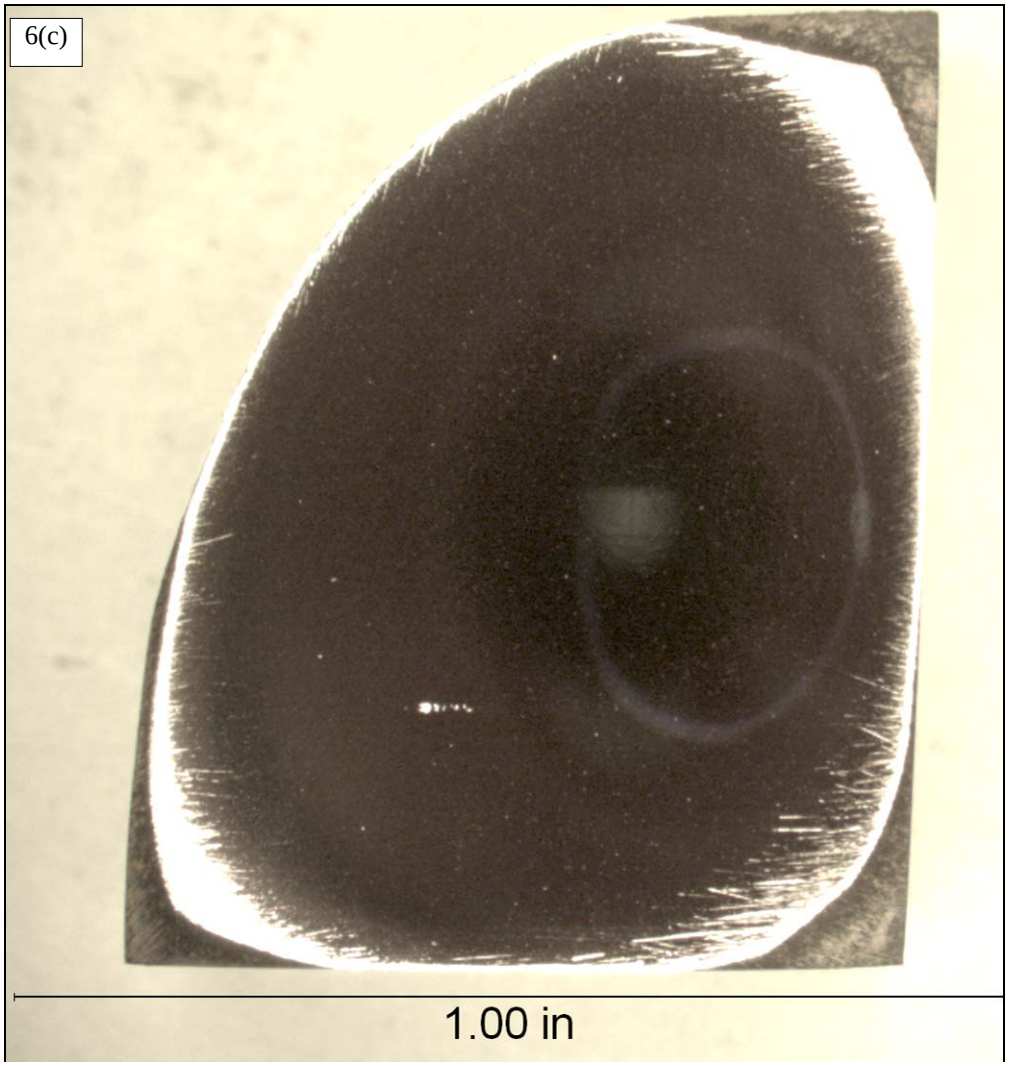

Figure A-7 shows macrographs with magnifications at 3.5x (Figure A-7(a)) and 45x (Figure A-7(b)) of the gage side of the laser-glazed rail removed from FAST after approximately 5.6 MGT of HAL traffic. Cracks were observed at the gage region within the glazed areas. The circled aras show the cracks on the glazed region and parent rail material. Comparing Figures A-7(a) and 7(b) with Figures A-5(b) through 5(d), it is clear that an increase in the severity of the damage observed in the gage corner of the rail increased under HAL traffic. The stereoscopic analysis further confirms the previously mentioned damage on the microstructure of the laser-glazed rail. In addition, not only were perpendicular cracks to the glazing region identified, but also the cracks going into the parent rail branched, resulting in a web of cracks. The branched cracks can act as stress concentrators that promote premature failure of the rail particularly under cyclic fatigue conditions. Figure A-6(b) shows that the samples extracted from the field side from the non-service and service-tested samples did not contain areas with cracks or other damage associated with the laser-glazing process.

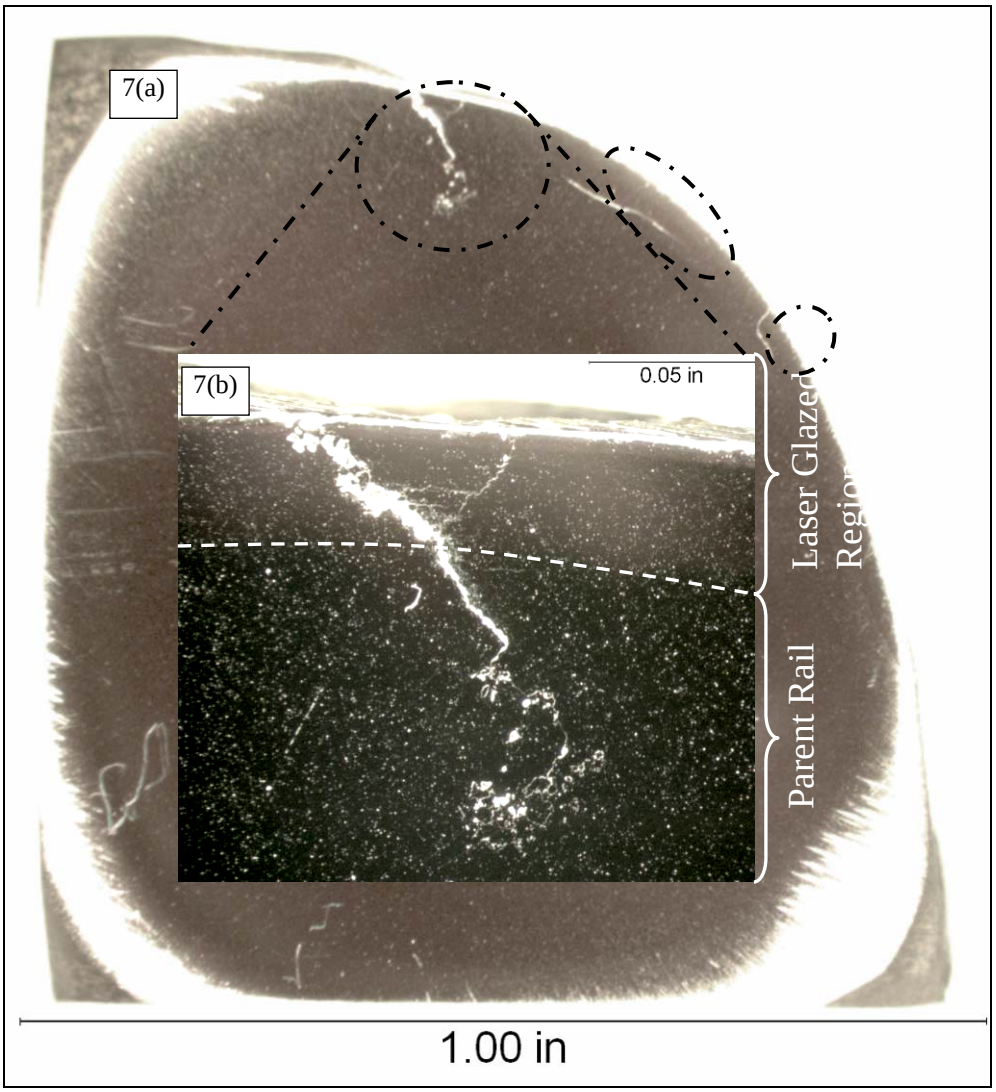

Figure A-7. Macrographs of the Laser-Glazed Treated Rail Removed from FAST After Approximately 5.6 MGT of HAL Traffic

A-3.2 Optical Microscopy Examination

The microstructures of the laser-glazed samples were observed under various magnifications on both the polished and etched samples. The etching reagent used was NITAL 2 percent for ~3 seconds at room temperature. The polished surface for the non-service tested (gage and field) microstructures contained a limited number of inclusions (probably sulphurs) visible at low and high magnification (Figures A-8(a) and 8(b) respectively). Figure A-8(c) shows the etched microstructure where various regions can be identified as in agreement with a previous report conducted on laser-glazed rails [Ref.1]. These regions contain martensite, amorphous areas (presumably the white zones in Figure A-8(c)), and, in the lower part of the sample, the unaffected (non-glazed) region showing the fully pearlitic structure.

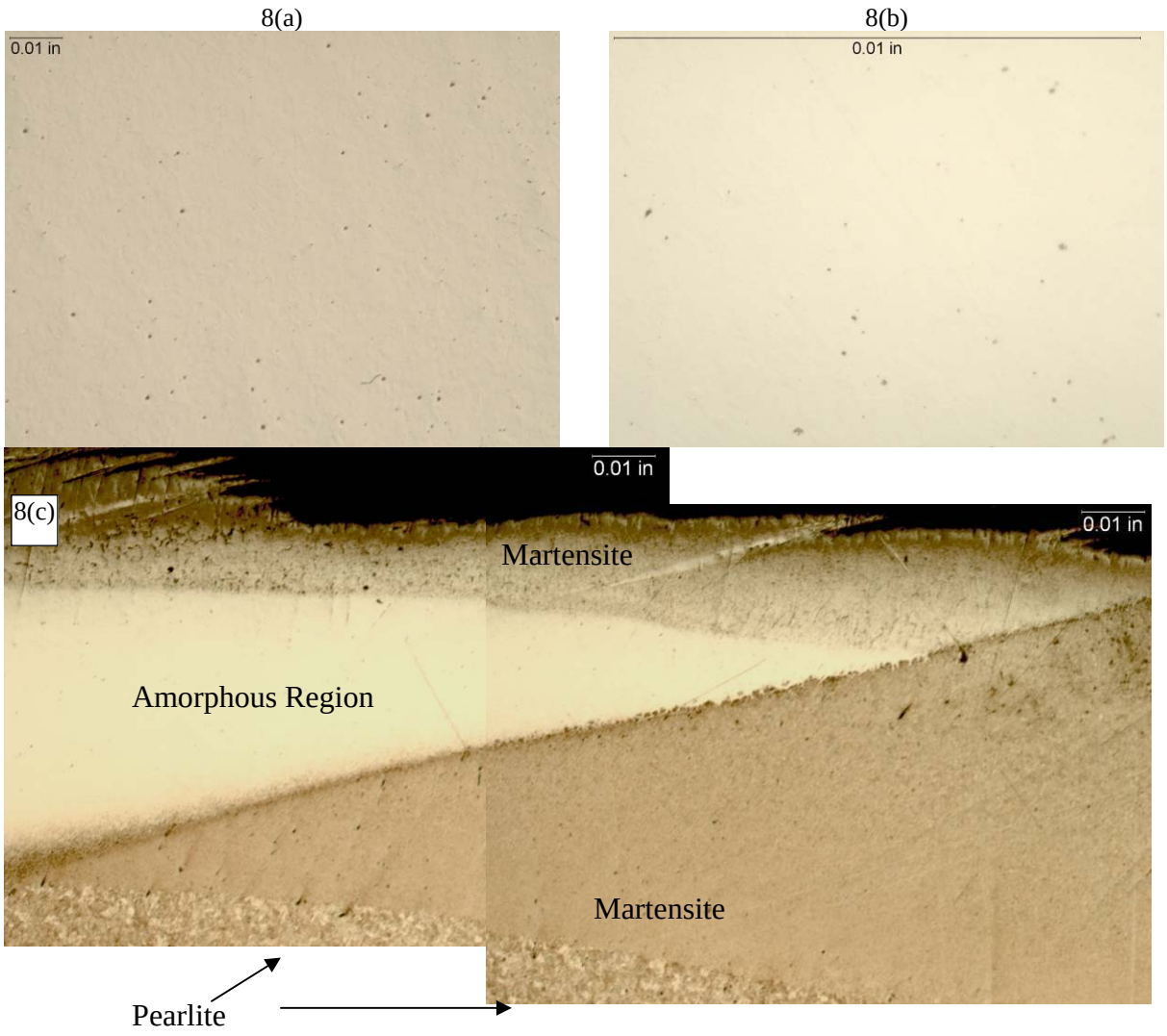

Figures A-8(a) and 8(b). Microstructure of the Laser-Glazed Region After Polishing.
Figure A-8(c). Micrograph of the Various Regions Observed at the Glazed Regions

Figure A-9 shows the etched microstructure of the glazed regions and parent rail material for the non-service tested rail. It shows the various microstructures presented by different zones of the rail in the glazed region (selected areas from Figure A-8). Figure A-9a shows the presence of martensite that is evident at magnifications of 200x and 500x. At 200x it can also be observed that the cracks end at the interface between the glazed region (martensite) and the unaffected parent material (pearlite; Figure A-9(b)). Figure A-9(c) shows overlapping of the two glazing treatments. Some porosity along the interface of both regions can be observed at 200x in (Figures A-9(b) and 9(c)). The porosity was presumably created during the glazing treatment and is detrimental to the integrity of the rail. Figure A-9(d) at 200x shows a fully pearlitic region found in the parent rail material.

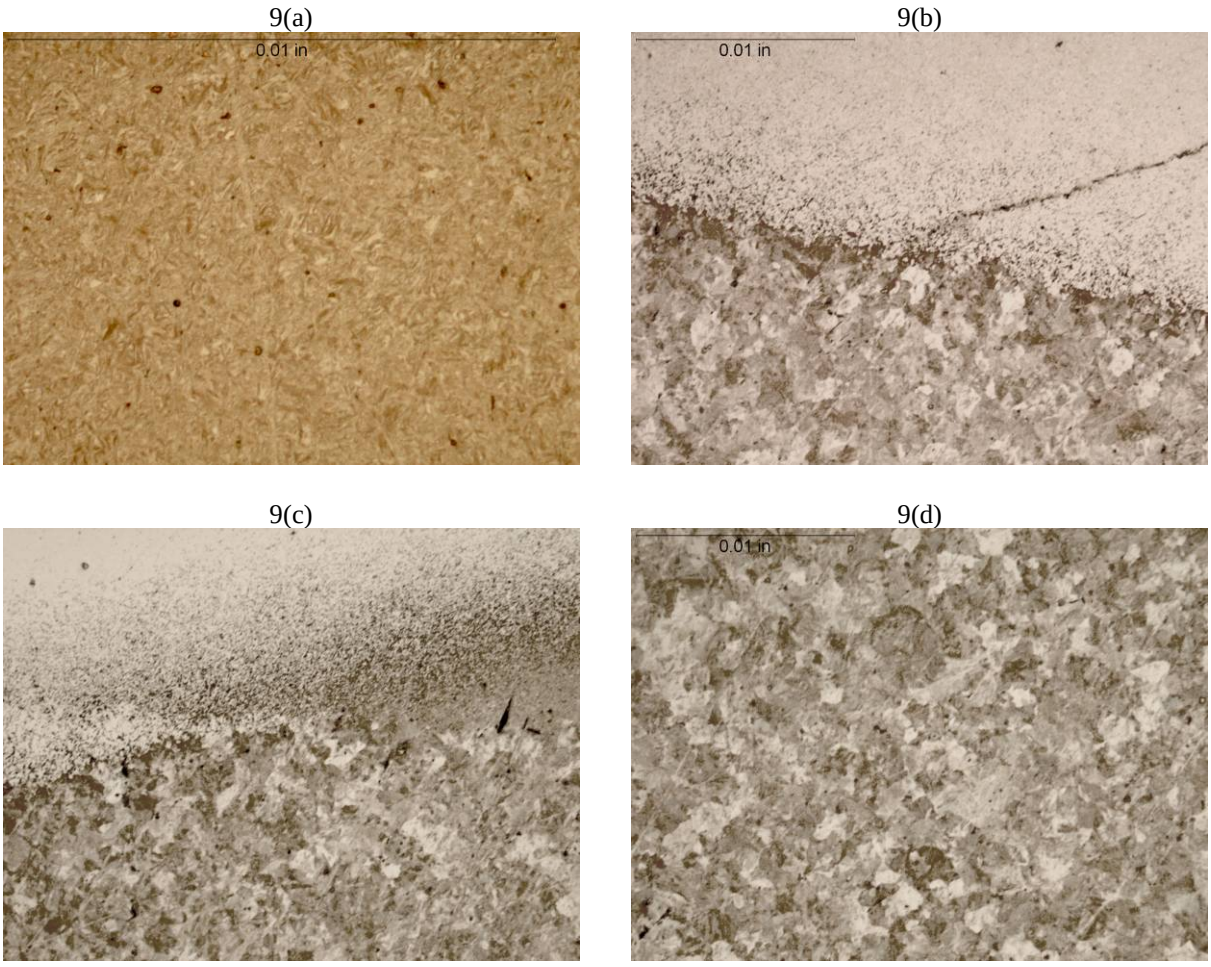

Figure A-9. Etched Microstructure of the Glazed Regions and Parent Rail Material for the Non-Service Tested Glazed Rail. Figure A-9(a). Martensite (500x). Figure A-9(b). Crack Stopped at Interface Between Glazed Region and Unaffected Parent Rail (200x). A-9(c). Overlapping of Two Glazing Treatments (200x). Figure A-9(d). Peralitic Region in Parent Rail Material (200x)

Figure A-10 shows the polished microstructures of the glazed region of the service-tested rail. The number, location, and severity of the cracks observed on the gage sides for the service-tested rail (5.6 MGT of HAL traffic at FAST) has increased considerably. For instance, Figure A-10(a) shows a crack that ended at the interface between the glazed region and the parent rail material and a crack that ramified into the parent rail material. Figure A-10(b) shows a crack along the glazed region of tested rail removed from FAST after approximately 5.6 MGT of HAL traffic. This crack was likely created from the shelling of the glazed treated surface under HAL traffic. Figure A-10(c) shows a crack across the laser-glazed region where both laser-glazed treatments overlap. In both ends the crack ramified (arrows indicate the interface). It is a good example of the possible residual stresses created due to the glazing treatment that created regions highly susceptible to cracks. This is further assisted by the martensite formation. The above-mentioned residual stresses promote susceptibility to crack formation, in particular to cracks in the gage surface and the interface between the glazed regions and the parent rail material. This accelerates the progress of shelling.

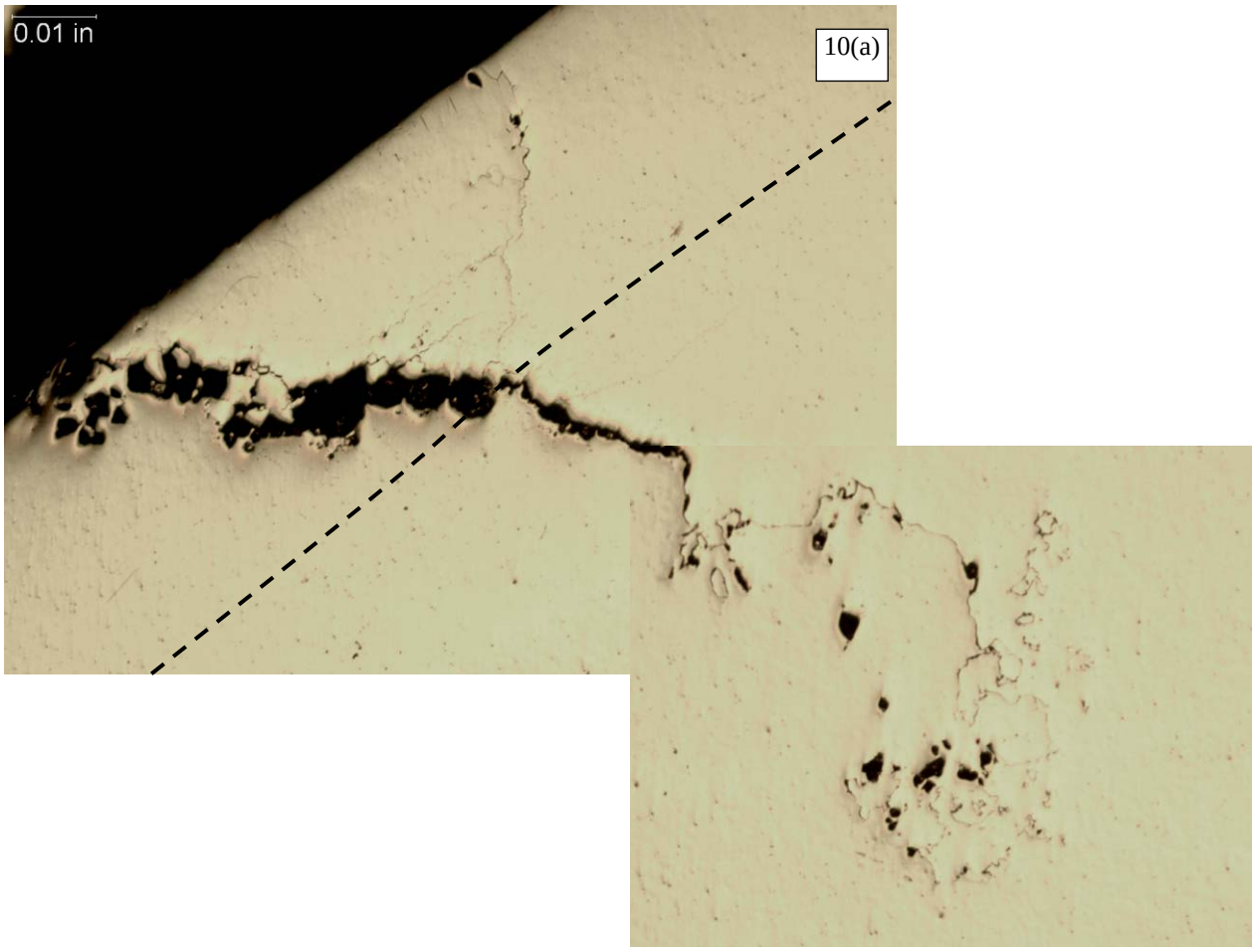

Figure A-10(a). A Crack Ending at the Interface Between the Glazed Region and Parent Material and a Crack that Ramified Into the Parent Rail Material

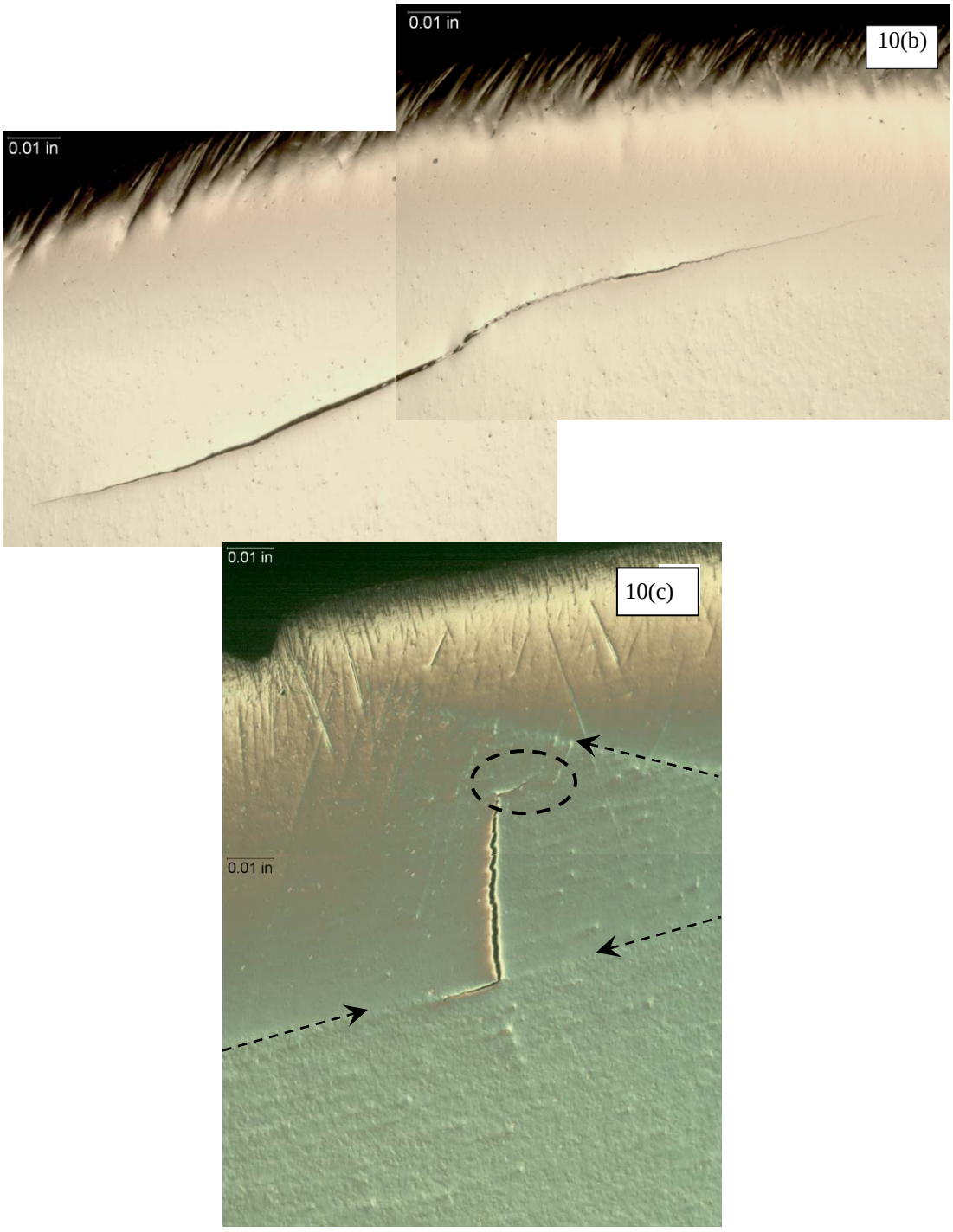

Figure A-10(b). A Crack Along the Glazed Region.
Figure A-10(c). A Crack Across the Laser-Glazed Region Where Both Laser-Glazed Treatments Overlap

Figure A-11 shows the etched microstructure of the glazed regions and parent rail materials for the rail removed from service after approximately 5.6 MGT of HAL traffic. Micrographs in Figure A-11 are magnified areas of the micrographs shown in Figure A-9(b) after etching. Figure A-11(a) shows micrographs on the etched microstructure of the various phases that form in the microstructure. The regions where sequential glazing treatments overlap present sections with sharp edges acting as stress concentrators. These build up stresses that can be detrimental and can compromise the integrity and service characteristics of the rail, resulting in crack formation (Figure A-11(b)). Figure A-11(c) shows sharp needles of lath martensite that formed at the interface between the glazed region and the parent rail material. The microstructure of the parent rail material is comparable to the non-glazed rail (field section) that is fully pearlitic.

11(a)

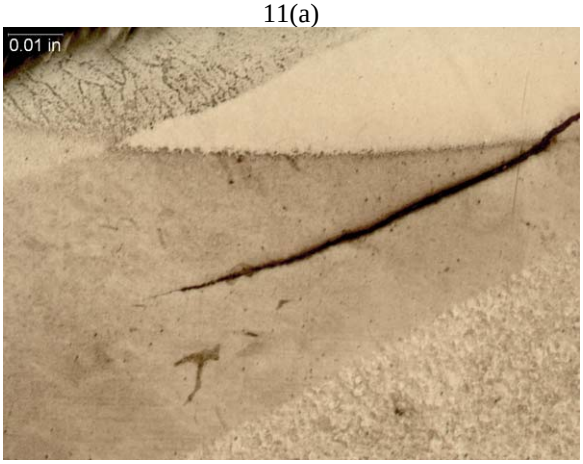

11(b)

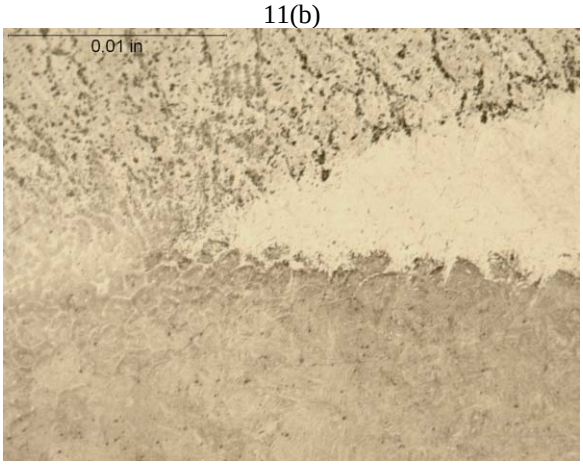

11(c)

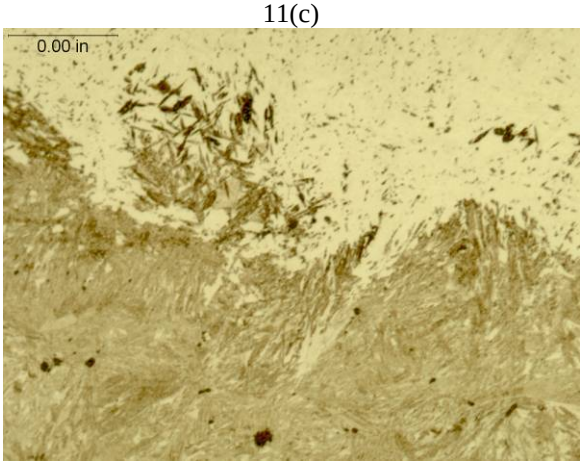

11(d)

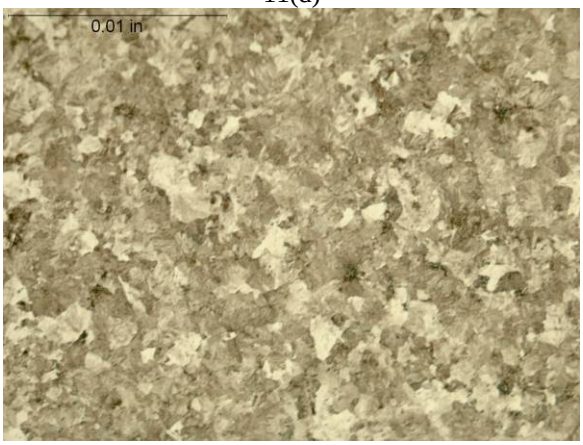

Figure A-11. Micrographs of the Etched Microstructure of the Service-Tested Glazed Rail.
Figure A-11(a). Affected Regions of the Rail by the Glazed Treatment (50x).
Figure A-11(b). Overlapping of Both Glazed Treatments (200x).
Figure A-11(c). Zones Showing Sharp Laths of Martensite (1,000x).
Figure A-11(d). Pearlitic Regions of the Parent Rail Material (200x)

Figure A-12 shows the microstructures of the rail's field sections. For the field regions, only a set of pictures for the non-service tested and the service-tested rails is presented since the microstructure in either case shows no significant differences under various magnifications up to 500x. After polishing, the microstructure shows a low amount of inclusions, probably sulphurs; on the other hand, the etched microstructure is fully pearlitic as expected.

12(a)

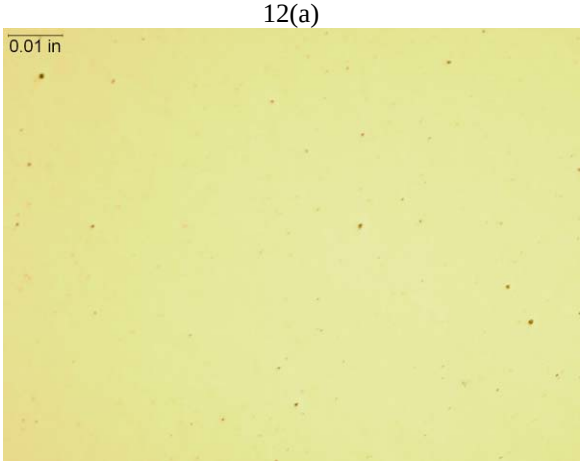

12(b)

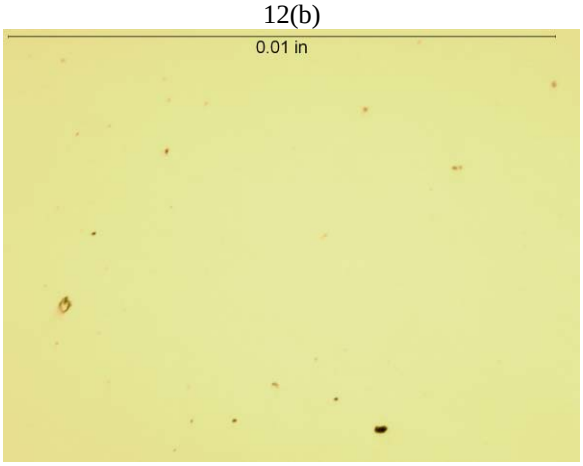

12(c)

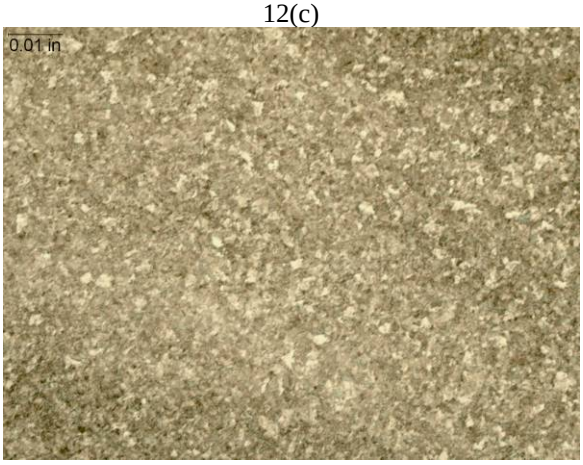

12(d)

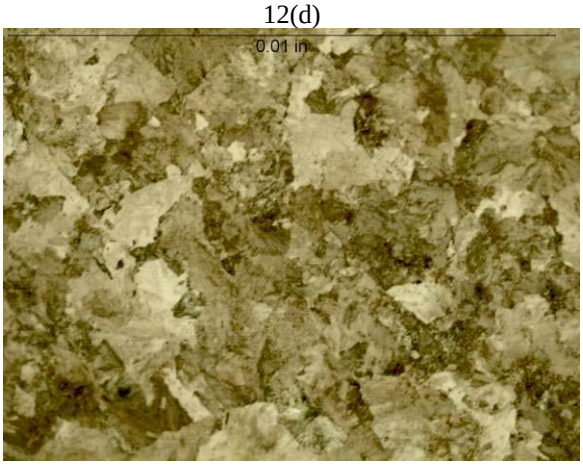

Figures A-12(a) and 12(b). Microstructure for the Laser-Glazed Rail Showing as Polished Surface.
Figures A-12(c) and 12(d). Etched Microstructure.
Figures A-12(a) and 12(c). 50x Magnification.
Figures A-12(b) and 12(d). 500x Magnification

A-3.3 Mechanical Testing

A-3.3.1 Micro-Hardness Test

Four specimens for non-service tested and service-tested rail conditions (two from the gage sides and two from the field sides, respectively) were tested for micro-hardness. The micro-hardness measurements were conducted, as shown in Figure A-13. The micro-hardness measurements at the edge (profile) of the sample for the field sections were conducted only for one non-service tested and one service-tested sample since the micro-hardness measurements were consistent. Table A-1 presents a summary of the micro-hardness measurements results and the statistical analysis of the results for the Left (L), Center (C), and Right (R) diagonals and the Edge (E) regions of the analytical samples. The micro-hardness of the gage of the rail (glazed-treated section) was very consistent and comparable to the micro-hardness obtained on the field side of the rail. The micro-hardness of the parent rail material averaged 414.1 ± 27.2 HV; for the gage (laser-glazed) region, the micro-hardness averaged 881.75 ± 92.1 HV. The higher standard deviation presented in the gage side along the glazed region is the result of the lack of integrity and homogeneity of the glazed regions that are mainly composed of amorphous [Ref. 1] and martensitic regions or zones.

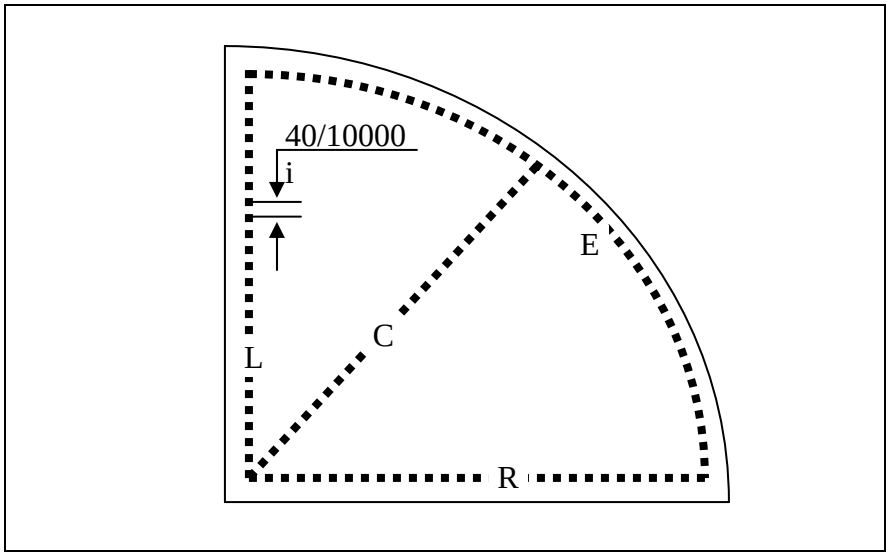

Figure A-13. Sketch of the Micro-Hardness Measurements as Conducted for the Tested and Non-Tested Sections of the Investigated Samples. The Micro-Hardness Measurements Were Conducted Along L, C, R, and E Regions

Table A-1. Results of the Micro-Hardness Analysis for the Gage and Field Samples Under Non-Service Tested and Service-Tested Conditions (for more detail see Figure A-13)

	Average (HV)	Standard Deviation (HV)	Confidence Limit (95%)	Confidence Limit (99%)
Non-Service Tested Rail "Field"				
Left	398.8	22.6	9.1	11.9
Middle	404.6	24.5	9.8	12.9
Right	385.8	40.3	16.1	21.2
Non-Service Tested Rail "Gage"				
Left	429.2	23.2	9.3	12.2
Middle	424.8	23.6	9.4	12.4
Right	418.1	21.6	8.6	11.3
Edge	857.1	56.3	29.6	29.6
Service-Tested Rail "Field"				
Left	418.4	26.4	10.6	13.9
Middle	421.7	23.2	9.3	12.2
Right	436.6	19.5	7.8	10.3
Edge	400.6	26.1	10.4	13.7
Service-Tested Rail "Gage"				
Left	404.8	18.9	7.6	9.9
Middle	420.5	27.3	10.9	14.3
Right	496.4	17.7	7.1	9.3
Edge	917.9	121.3	48.5	63.4

A-3.3.2 Charpy Test

Six specimens (three from the gage and three from the field side) for non-service tested and service-tested conditions were extracted and machined according to the E370 American Society for Testing and Materials (ASTM) standard. Impact charpy tests were carried out at various temperatures (-30° C (5° F), 0° C (32° F), and 65° C (175° F)) to investigate the effect of the glaze treatment on the fracture mechanism for the steel at extreme temperatures for revenue service. Table A-2 shows the results of the energy absorbed by the sample during the impact (charpy) test. From Table A-2, it can be concluded that the energy absorbed during the impact test increased with temperature, which is expected; nonetheless, all fractures observed were brittle with limited deformation presented by the samples (Figure A-14). Figures A-14(a) (field) and 14(b) (gage) are non-service tested conditions. The above-mentioned increase in energy (for the samples extracted from the field regions) is more indicative that the glazed treatment reduced the impact toughness. Furthermore, the affected regions with the internal damage are severe, resulting in one of the samples fracturing away from the notch region (Figures A-14(c) and 14(d)). Figure A-14(d) has a dotted line that circles the notch of the sample. Severe damage was caused during the machining of the notch due to the high brittleness probably created by the martensite. Results suggest that the glaze treatment can form stress concentrations considerably larger than the ones created by the engineered notch typically machined for the charpy samples.

Table A-2. Results of the Charpy Test Conducted for Samples Extracted from the Gage (Glazed) and Field Regions for Non-Service Tested and Service-Tested Conditions

Sample/Testing Temperature	Absorbed Energy in Ft^2/Pound		
	-30° C (5° F)	0° C (32° F)	65° C (175° F)
Non-Service Tested	3.8 (gage) 4.2 (field)	5.0 (gage) 5.5 (field)	5.7 (gage) 8.0 (field)
Service-Tested	3.5 (gage) 4.5 (field)	4.3 (gage) 5.75 (field)	6.0 (gage) 8.5 (field)

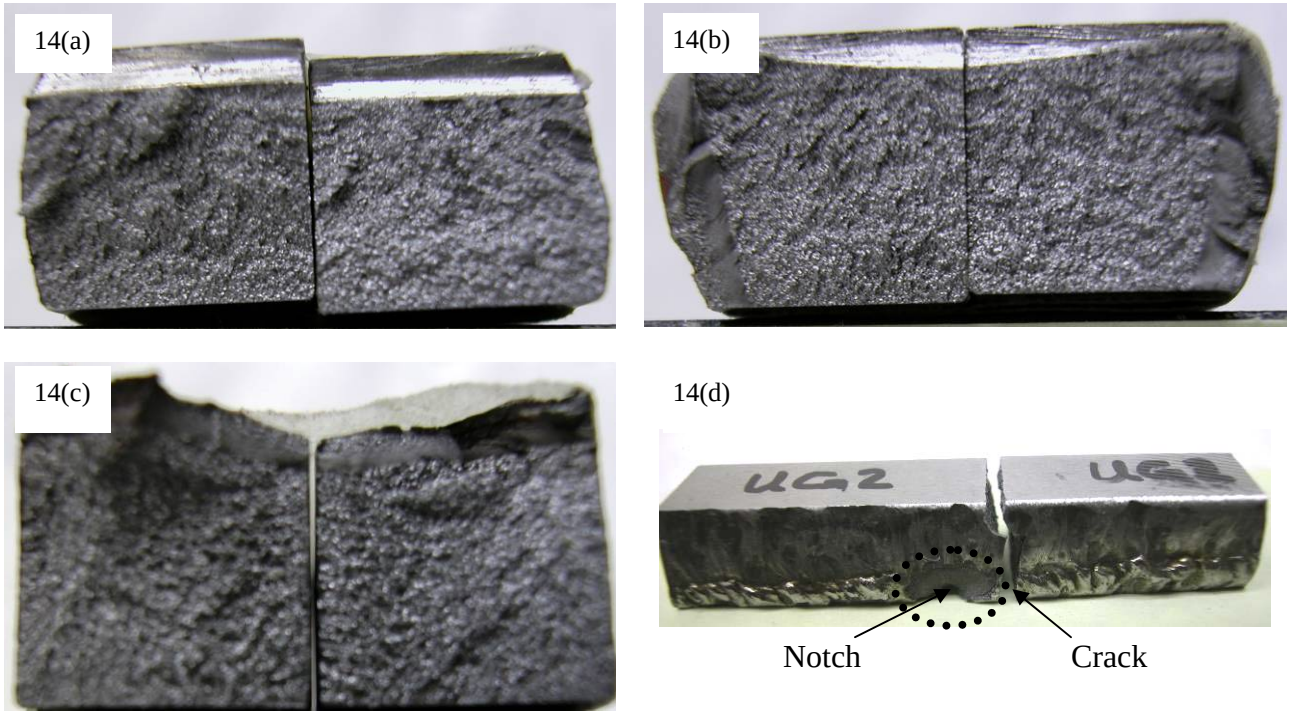

Figure A-14. Pictures of Selected Charpy Tested Samples Showing Fresh Fractures

A-4.0 Conclusions

The use of laser-glazing technology for the railroad industry as a substitute for rail lubrication is an interesting prospect that requires further investigation. The possibility of reducing the roughness of rail at the gage corner by creating a hard surface would reduce the friction between the rail and the wheel. This has a potential application to reduce or eliminate the use of lubricants for revenue service in curves. Nonetheless, the current technique is only capable of reducing the roughness in a discrete manner rather than continuously (see Figures A-1b and A-1(c) for details). In addition, the integrity and service characteristics of the glazed regions compromise the survivability of this type of treated rail in revenue service.

For many applications, wear is associated with the hardness of the material; however, previous reports by TTCI [Ref. 2] showed that this is not necessarily the case. In fact, the mechanisms that influence the different phases to deform and fracture are as important for wear resistance, integrity, and service characteristics as the materials themselves. The present analysis is a good example, since the transformation of pearlite to martensite by the laser-glazed treatment is simple since martensite is considerably harder than pearlite. However, the transformation of austenite, which is the face cubic centered phase that is found at temperatures between ~800° C (~1,550° F) and ~1,200° C (2,200° F), for the investigated alloy to martensite by a rapid cooling is conducted by shear. This sheer creates residual stresses. The residual stresses in the overlap of both treatments could be in tension or compression, resulting in areas or regions that are sensitive to crack formation and aid crack propagation (see Figures A-10(c) and A-14).

Sawley, in Reference 1, mentions that the laser-glazed treatment can increase the rail's temperature well up into the austenitic region (~900° C or ~1,650° F). The characteristics of the treated glazed rail tested in service for the present analysis, however, show a surface with the typical characteristics of a re-melted material. This may indicate that the temperature reached by the rail's surface during the glazing treatment was considerably higher, in the range of the semi-solid or liquid state temperatures (>1,200° C (2,200° F) for this alloy).

The heat affected zone is well localized into the glazed region and makes this treatment worth further study, since the parent rail material (fully pearlitic microstructure) appears to be un-affected (compare the microstructures and micro-hardness of the pearlitic regions for gage and field regions in Figures A-9 through A-11). The above argument further confirms the reasons for the abrupt increase in micro-hardness from less than 440 HV to more than 1,000 HV in a distance of less than 0.001 inch (interface).

A-5.0 Recommendations

It is recommended that all laser-glazed treated rails undergo a full metallurgical evaluation to determine their integrity before their use in revenue service. It is suggested that no glazed rail presenting the characteristics of the samples investigated at TTC be subjected to service traffic, either at FAST or revenue service. This recommendation does not include the elimination of the laser-glazed treatments for standard and/or premium rails but rather encourages the optimization of the technique. An optimized technique would ideally heat treat the rail's surface by heating the rail to the austenitic temperature, avoiding an overheat of the rail that could reach the semi-solid or liquid states. This would keep intact the integrity of the rail's surface, minimizing or eliminating cracks and residual stresses. The treatment that is proposed would transform a small region of the surface into bainite, martensite, or a combination of phases and at the same time form a smooth hard shell. This, however, raises the following questions that will help to further optimize the laser-glazed technique:

- Is a harder phase (other than pearlite) the alternative to maximize the wear life of the rail?
    - If so, why did steels like J6 steel (fully bainitic [Ref. 2]) not perform as expected under HAL service traffic operation at FAST?
- What will happen once the laser-glazed treated surface wears out?
- Will the higher hardness of the laser-glazed treated rail wear the wheels more rapidly?
- Is there a methodology to glaze the rail in-track for revenue service?

A-6.0 References

1. Sawley, K. and J. Sun, "Laser Glazing to Reduce Rail Wear," *Technology Digest* TD-97-024, Association of American Railroads, Transportation Technology Center, Inc., Pueblo, CO, July 1997.

2. J. Kristan, "FAST Rail Evaluation Test–Fracture Performance and Discussion," *Technology Digest*, TD-05-024, Association of American Railroads, Transportation Technology Center, Inc., Pueblo, CO, October 2005.

3 Welsch, G.E., "Iron–Carbon/Cementite Phase Diagram," ASM International, Materials Park, OH, 1994.

Appendix B.
Nuvonyx Laser-Glazing of Rail for AAR/TTCI FAST Loop Tests

Nuvonyx, Inc.
3753 Pennridge Drive
Bridgeton, MO 63044
www.nuvonyx.com

Local: 314.209.7755
Toll Free: 877.209.7755
Fax: 314.209.1728

Report Date: October 12,2005

Nuvonyx, Inc. Processing Report: Laser-Glazing of Rail for AAR/TTCI FAST Loop Tests

Contract No. 5F-00545, Nuvonyx, Inc. W.O. #15080

Contract Task 1: *Perform all necessary scoping tests to identify proper laser-glazing conditions to produce a laser-glazed segment on the gage/top segment of the 40 foot long rail segment. The size of the glazed region shall be approximately 1" wide. The treatment depth shall be a minimum of 1-1/2 mm deep. In developing the protocols, attention should be given to the fact that a portion of the 1" wide track may extend from the flat gage face up onto the curved top of the rail e.g. the region to be glazed will contain a curved surface. Approximately ½" of the 1" width will extend beyond the gage point up onto the top of the rail. (See attached schematic/*sketch). Schematic/Sketch Shown Below as Schematic / Sketch No. 1

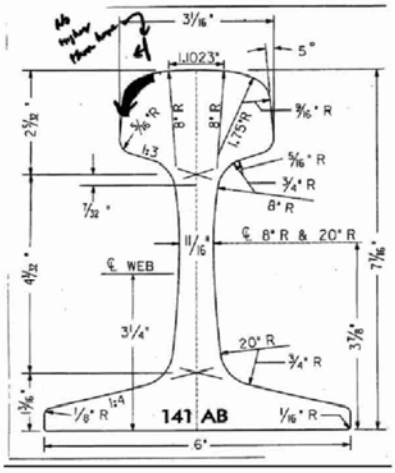

Schematic / Sketch No. 1

Task 1: Implementation By Nuvonyx, Inc.:

Sample laser glazing segments (tracks) were ran on a test specimen to identify proper laser-glazing conditions required to achieve a laser-glazed segment with the required width of 1" and required minimum treatment depth of 1-1/2 mm. Nuvonyx, Inc. received the test specimen rail with white paint marker on one end indicating the area required to be glazed. This marking corresponded to the black markings on Schematic / Sketch No. 1 shown on page 1 of this report. This area was used on the test specimen to develop the parameters for use on the 40' rail section.

Watts	Speed	Focal Length	Comments
3500	.5 Meters / Minute	94mm	Too fast / power. Cannot meet the 1-1/2 mm depth requirement
3500	.6 Meters / Minute	94mm	Too fast / power. Cannot meet the 1-1/2 mm depth requirement.
3500	.8 Meters / Minute	94mm	Too fast / power. Cannot meet the 1-1/2 mm depth requirement.
3800	.4 Meters / Minute	94mm	Appears too slow / power. Excessive Melt Observed.
3800	.5 Meters / Minute	94mm	Best appearance of all tracks. Most consistent. Meets 1-1/2 mm depth requirement.
3800	.6 Meters / Minute	94mm	Looks similar to 3800 Watts @ .5 Meters / Minute but looks marginal on capability to meet the 1-1/2 mm depth requirement.
3800	.8 Meters / Minute	94mm	Too Fast / power. Cannot meet the 1-1/2 mm depth requirement.

Table 1: Initial Test Track Parameters

As can be seen in the following photographs the rail section was placed large steel layout tables. A Bug-O carriage and track system was placed beside the rail section and aligned both horizontally and vertically to the rail.

It was determined that the rail would need to be placed in 2 different positions in order to achieve the approximate 1" wide glazing area required. The two positions are No.1 upright and No.2 laying down on it's side as shown in Photographs 1 and 2 respectively.

With the rail sitting in position No. 1, upright, flat on the table in the orientation it would be tied into an actual track, the end of the 40 foot sections where flat on the table. At the center of the rail, where the weld joint was, the rail was appoximately1/2" higher than the ends. The bulk of the 1/2" run out was within 6 feet either side of the thermite weld. The Bug-O track was shimmed in the center to run parallel with the rail when processing in the upright position. When the rail was set in position No. 2, laying down on it's side as shown in Photograph No. 2, the Bug-O track was adjusted to keep the run-out perpindicular to the bow in the rail.

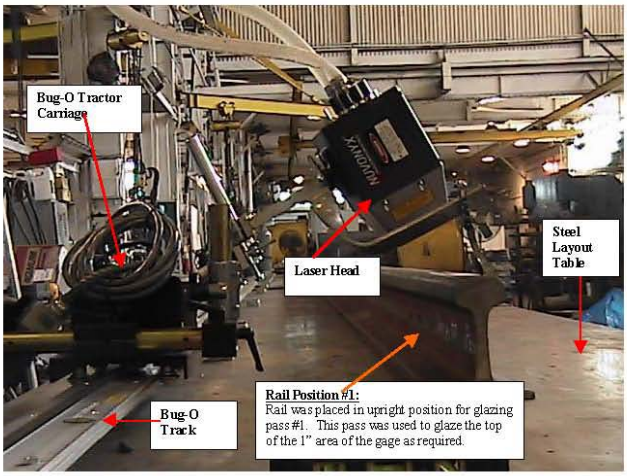

Photograph 1: Rail Upright Configuration

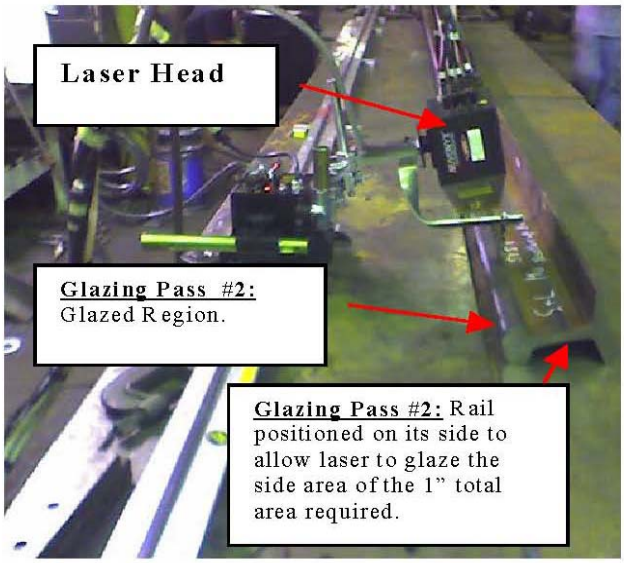

Photograph 2: Rail On Side Configuration

As shown in Photograph 3. Dye Penetrant testing was used on preliminary test glazing passes to check for cracks. There were no cracks observed.

Photograph 3: Dye Penetrant Testing Single Tracks

Photograph 4: Dye Penetrant Testing Of Overlapping Sections

Photographs 5 & 6 show test specimens that were cut and etched to determine the depth of treatment.

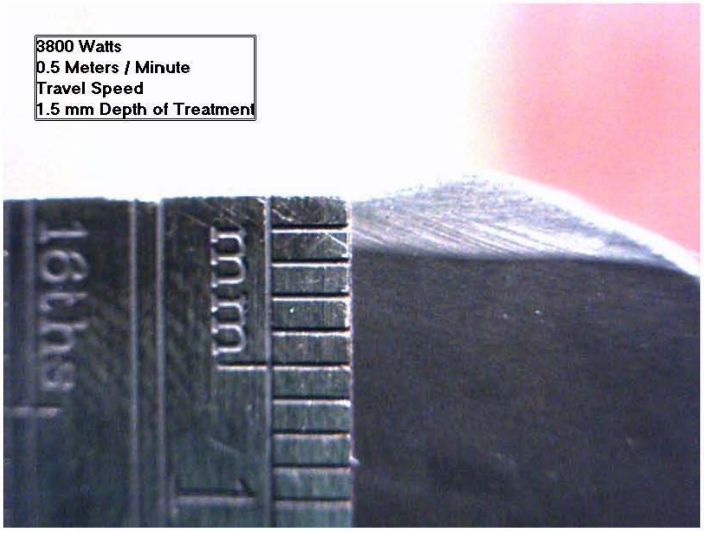

Photograph 5: Cross Section of Glazed Section Required 1-1/2 mm Treatment Depth.

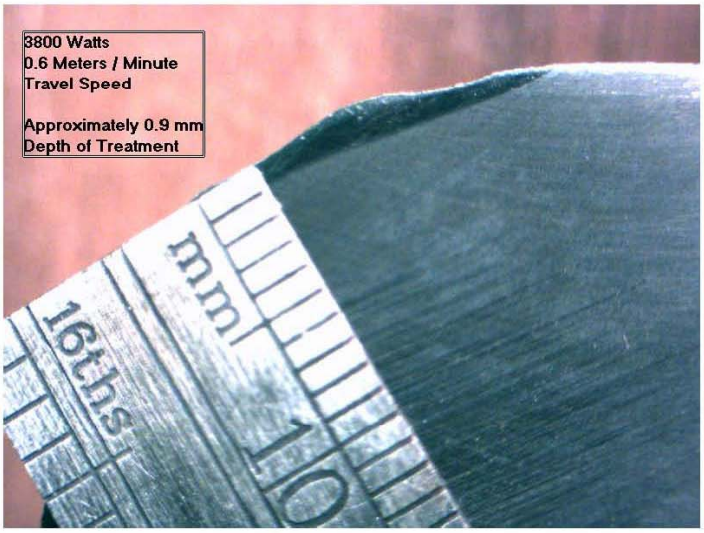

Photograph 6: Cross Section of Glazed Section

Photograph 7 shows the width of the laser glaze at 1" wide when using the parameters of 3800 Watts, .5 Meters/minute travel speed and 94mm focal length. This requires two overlapping tracks.

Photograph 7: 1" Glaze Width

Contract Task 2: *Laser glaze a 1" wide strip down the entire length of the 40 foot long segment.*

Task 2: Implementation By Nuvonyx, Inc:

Once the proper laser-glazing parameters were established from Task #1, the full 40' long segment was glazed. The 40' section of rail was received without any marking showing the area to be glazed. As noted above in "Task 1: Implementation By Nuvonyx, Inc.", the 4' test specimen was received with the glazing area marked. The marking from the 4' test specimen was used as a guide to locate the area to be glazed on the 40' section.

In order to ensure the laser head remained steady and at the right focal length of 94mm, a standoff roller-wheel was fabricated. The roller wheel is shown in photograph 8.

Photograph 9 shows the 40' section during the process of Laser Glazing and Photograph 10 shows the rail section after completion of the Laser Glazing.

Processing Parameters used were as follows:

- 3800 Watts
- .5 Meters / Minute
- 94 mm Focal Length

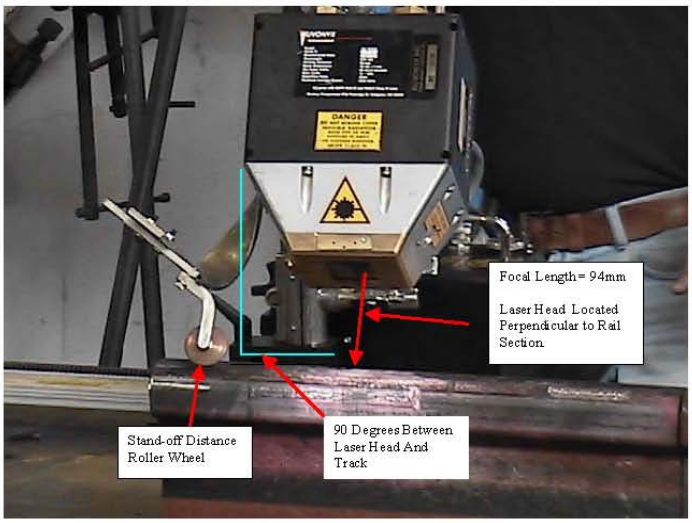

Photograph 8: Rail With Laser Head And Roller Wheel.

Photograph 9: In Process Gazing of Entire 40' Section.

Photograph 10: Completed Rail Glaze

Contract Task 3: *Perform all necessary QA on the glazed rail segment to ensure glazing uniformity and integrity.*

Deliverable – Copies/documentation related to QA of the glazed rails (metallography, mag-flux, hardness, etc.).

Task 3: Implementation By Nuvonyx, Inc.:

As shown in photograph 7, the glazed section was measured to ensure the glazed region was "approximately 1 inch" wide.

- As shown in photographs 5 & 6, the preliminary test specimen rail was checked by cross sectioning, etching and measuring, to ensure the parameters used for glazing the 40' rail section would produce the required treatment depth minimum of 1-1/2 mm deep.

- The entire glazed section of rail was checked for cracks by using the Dye Penetrant method of inspection. Cracks were found along the entire length of the rail in the pass one area of the glaze. Photograph 11 shows the type of cracking that was found along most of the length of the rail section. Although the center of the rail section appeared to have some slight indications of cracking, the indications were less than (as can be seen in Photograph 12) the indications observed on the rest of the rail. It should be noted that the center section of the rail is where the rails had been previously welded together and ground smooth. The rest of the rail had mill scale on it. It was cleaned with a power wire brush prior to the laser glazing process.

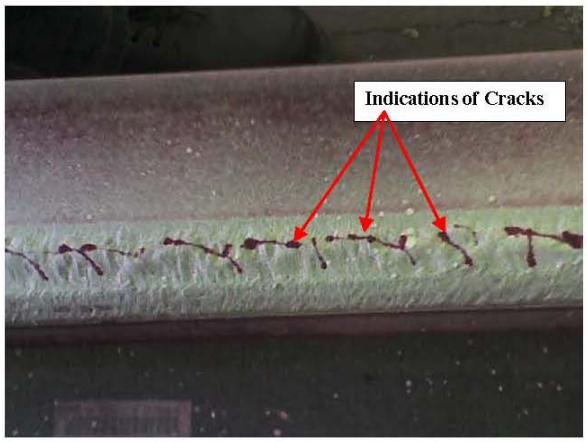

Photograph 11: Dye Penetrant Inspection of 40' rail section.

Photograph 12: Dye Penetrant Inspection Showing Center Section of Rail With Clean Ground Surface.

Contract Task 4: *Return rail to AAR/TTCI for testing (shipping costs to be covered by TTCI).*

Task 4: Implementation By Nuvonyx, Inc.:

The rail was picked up by a TTCI contracted trucking agency at approximately 3:45 PM, Thursday, October 6, 2005. A scanned copy of the shipping ticket is shown below.

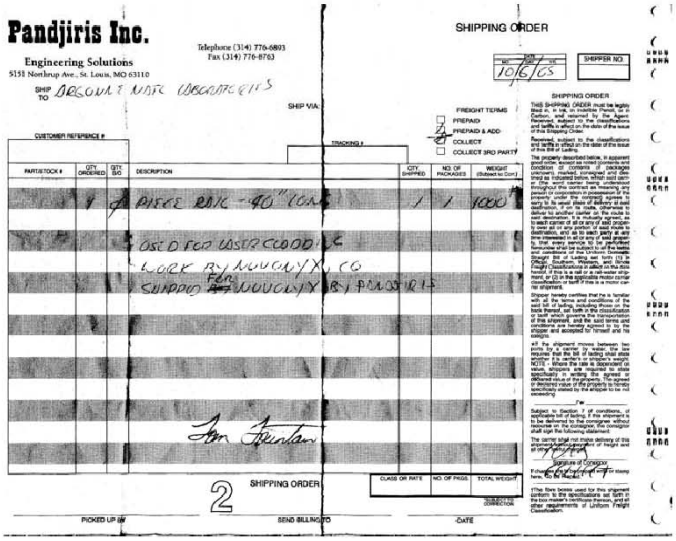

Pandjiris Inc.

Engineering Solutions

5151 Northrup Ave., St. Louis, MO 63110

Telephone (314) 776-6803

Fax (314) 776-8763

SHIPPING ORDER

SHIPPER NO.

10/6/05

SHIP TO ARGONNE NATL LABORATORIES

SHIP VIA

FREIGHT TERMS

PREPAID

PREPAID & ADD

COLLECT

COLLECT 3RD PARTY

CUSTOMER REFERENCE #

TRACKING #

PART/STOCK #	QTY. ORDERED	QTY. B/O	DESCRIPTION	QTY. SHIPPED	NO. OF PACKAGES	WEIGHT (Subject to Corr.)
	1		PIECE RAIL - 40" LONG	1	1	1000
			USED FOR USER CODDLING			
			WORK BY NUVONYX, CO			
			SHIPPED FROM NUVONYX ARGONNE IL			

SHIPPING ORDER

2

CLASS OR RATE | NO. OF PKGS. | TOTAL WEIGHT

PICKED UP BY | SEND BILLING TO | DATE

Scan Document No. 1

Nuvonyx, Inc. Project Complete

Completed Processing Schedule

- Rail Received At Pandjiris: 9/26/05
- Nuvonyx, Inc. Site Preparation & Setup: 9/28 & 9/29/05
- Nuvonyx, Inc. Rail Processing: 9/30/05
- Nuvonyx, Inc. Site Tear Down: 10/1/05
- Rail Shipped Back to AAR/TTCI: 10/6/05

If you have any questions regarding any of this information please contact our office at your earliest convenience.

Sincerely,

Kevin Laughlin

Acronyms

DOE Department of Energy

FAST Facility for Accelerated Service Testing

FRA Federal Railroad Administration

HAL heavy axle load

HH heat-treated head hardened rail

HTL High Tonnage Loop

MGT million gross tons

TTC Transportation Technology Center (the facility)

TTCI Transportation Technology Center, Inc. (the company)